

# Vista: Vector Indexing and Search for Large-scale Imbalanced Datasets

Yujian Fu\*, Cheng Chen<sup>†</sup>, Yao Chen\*, Weng-Fai Wong\*, Bingsheng He\*

\*National University of Singapore, <sup>†</sup>ByteDance Inc

{yujianfu, wongwf, hebs}@comp.nus.edu.sg, yaochen@nus.edu.sg, chencheng.sg@bytedance.com

**Abstract**—With the rise of machine learning models, particularly generative models like sequence-to-vector models, there is a high demand for constructing efficient approximate nearest neighbor search (ANNS) indexes on the embedding vectors they generate. Despite the development of numerous indexes for efficient vector retrieval, the complex distributions of vectors generated by these models and their impact on ANNS tasks remain underexplored. In this work, we address the challenges faced by current advanced ANNS approaches when dealing with vectors characterized by imbalanced distributions, which negatively impact search efficiency. We identify the difficulty in indexing and searching certain vectors using previous ANNS graph indexes due to skewed distributions and propose a novel index, Vista, that improves efficiency by introducing dynamic index construction patterns based on vector distribution. Our experimental evaluation confirms Vista’s efficiency advantage, demonstrating that on both public and industrial-grade real-world imbalanced datasets, Vista achieves several to tens of times performance improvement compared to advanced ANNS indexes while ensuring high search accuracy and good scalability.

## I. INTRODUCTION

$k$ -Nearest Neighbor ( $k$ -NN) search is a fundamental task in numerous machine learning algorithms and serves as the foundation for various real-world applications such as information retrieval [37], machine learning [14], and recommendation systems [54]. With the emergence and success of large language models (LLMs) [4], [12], [36], [48], [49], nearest neighbor search has gained even more importance as a necessary component in the retrieval-augmented generation (RAG) [13], [16], [53] process. However, the curse of dimensionality [10], [27] makes vectors in high-dimensional space more indistinguishable, leading to unaffordable time costs for exact  $k$ -NN queries in modern applications. Consequently, researchers have turned to approximate solutions, trading some search accuracy for efficiency, a practice known as approximate nearest neighbor search (ANNS) [32], [33], [35], [52]. At ByteDance, achieving high accuracy and throughput in ANNS retrieval is essential for delivering precise and timely recommendations, advertisements, and risk control in large-scale, real-time applications.

Imbalanced vector distribution is a common phenomenon in ANNS datasets [11], [50], [51]. At ByteDance, we observe that embedding vectors generated by widely-used sequence-to-vector models, such as graph neural networks (GNN) [24], [26], [56] and generative pre-training models (GPT) [48], often exhibit strong imbalanced clustering properties. Examples are presented in Figure 1.

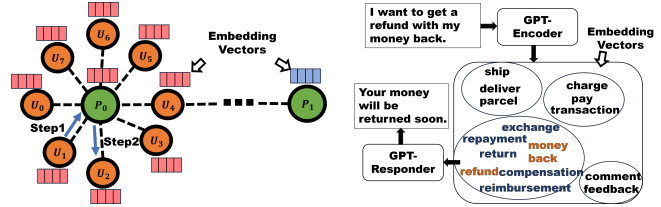


Fig. 1: Left: GNN embedding vectors bring popular products and nearby users closer together while increasing the distance to unpopular products. Right: GPT embedding vectors cluster together based on their semantic similarity.

The left figure presents the random walk GNN algorithm, which is widely used in e-commerce recommendation systems (e.g., Node2Vec [24], DeepWalk [47], LINE [56], etc.). We connect users ( $U_0 - U_7$ ) to purchased products ( $P_0, P_1$ ). Starting from a source point ( $U_1$ ), the GNN random walk generates sequences (e.g.,  $U_1 \rightarrow P_0 \rightarrow U_2$ ), forming positive pairs (e.g.,  $(U_1, P_0), (U_1, U_2)$ ) and selecting unconnected points as negatives (e.g.,  $P_1$ ). The algorithm clusters embeddings of positive pairs closer and pushes negatives farther away. In e-commerce, popular products ( $P_0$ ) attract many users, forming dense clusters, while niche products ( $P_1$ ), bought by few, have sparse, distant embeddings.

The right figure demonstrates the GPT-based language model used in chatbots. Given the input sentence ‘I want to get a refund with my money back,’ the GPT-Encoder tokenizes it and generates embeddings for each word. Words like ‘refund’ and ‘money back’ form a dense cluster due to frequent co-occurrence, along with related terms like ‘exchange,’ ‘repayment,’ and ‘return.’ In contrast, words related to Payment (e.g., ‘charge,’ ‘pay’) and Delivery (e.g., ‘ship,’ ‘deliver’) form different separate clusters, reflecting their semantic similarity. The GPT-Responder uses the dense cluster around ‘refund’ to generate a response like ‘Your money will be returned soon.’ This example highlights the clustered distribution of GPT embeddings, where similar terms group together based on their semantic context.

To understand the differences in distribution within ANNS datasets, we provide visualizations for four ANNS datasets from different sources in Figure 2, including SIFT vectors [38] for images, GoogleNET embedding vectors [55], text embedding vectors from Glove [46], and graph embedding vectors from LINE [56]. The dimensionality of the vectors is reduced to two using the  $t$ -distributed stochastic neighbor

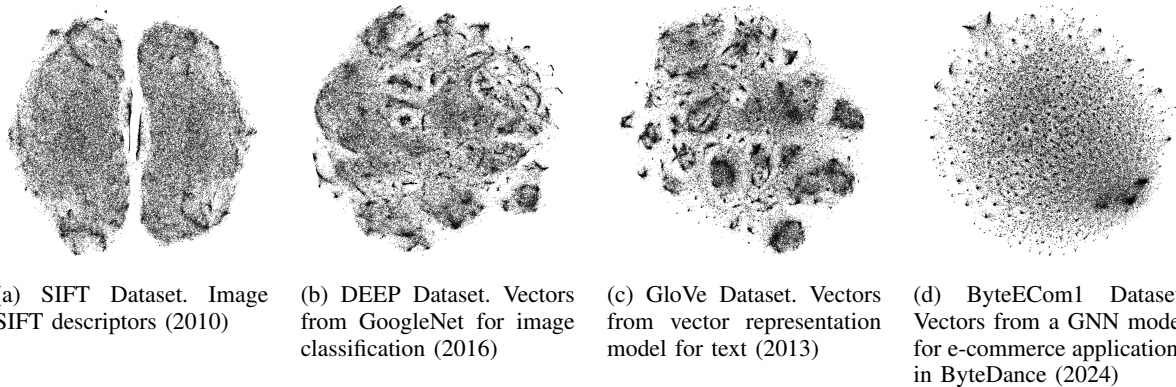


Fig. 2: Vector visualization of four ANNS datasets with  $t$ -SNE for dimensionality reduction. Each figure samples 100,000 vectors. We observe that vectors in the ANNS task follow imbalanced distributions, forming both dense and sparse areas. Recent datasets, especially embedding vectors from sequence-to-vector models such as GloVe and ByteECom1, have become more skewed and generate more local small clusters.

embedding ( $t$ -SNE) [58] method, which preserves the nearest neighbor relationships between vectors. One important observation from the figure is that embedding vectors are becoming more complex, with more small local clusters, resulting in a more imbalanced distribution among the vectors. This outcome aligns with the nature of generative models based on the skip-gram model [43], which seeks to make similar items close to each other, ultimately forming groups of closely related items in various clusters within high-dimensional feature spaces. With the success of generative models for graph and text data, handling such imbalanced datasets with numerous local clusters becomes essential for large-scale ANNS tasks.

Some studies [11], [50], [51] discuss the impact of skewness in data distribution on ANNS tasks. However, such imbalanced vector distribution is rarely addressed by advanced ANNS indexes. Recent ANNS benchmarks [8], [9], [33], [59], [61] demonstrate that graph-based ANNS indexes [19], [25], [39], [40], [60] are the top performers in terms of search quality and speed, achieving high recall and throughput through fine-grained control of search paths. They deliver search speeds magnitudes faster than other ANNS methods, such as inverted indexes [30] and hashing [57], [63]. Despite extensive efforts to optimize graph structures, the impact of vector distribution on ANNS—particularly in graph index construction and retrieval performance—remains underexplored.

$k$ -NN Connectivity	10	50	100	200
SIFT ( $\times 10^2$ )	8.17	6.82	6.39	6.16
DEEP ( $\times 10^3$ )	1.68	0.72	0.61	0.58
ByteECom1 ( $\times 10^4$ )	3.73	1.48	0.59	0.33

TABLE I: Vector search cost, represented by the number of distance calculations to find the vector on Vamana index [29], with respective to vector distribution, represented by  $k$ -NN connectivity on three datasets with 1 million vectors. We find vectors with lower  $k$ -NN connectivity are much more difficult to search. Detailed analysis is presented in Section III.

In this paper, we explore the imbalance in vector datasets and its impact on graph index structure and performance in

ANNS tasks. This is the first study, to our knowledge, that bridges the skewness of dataset distribution with the search efficiency of ANNS indexes. We find that points with low in-degree in a  $k$ -NN graph, referred to as points with low  **$k$ -NN Connectivity** are much more difficult to discover in traditional ANNS indexes and pose a significant obstacle to achieving high recall on large-scale datasets, as shown in Table I. From the table, vectors with  $k$ -NN connectivity of 10 require significantly more distance calculations, sometimes over 10 times the search cost of other vectors.

However, advanced graph indexes [29], [41], [44], [64] ignore differences in vector distributions during index construction and use a fixed configuration for all vectors, making them inefficient at searching for these points with low  $k$ -NN connectivity. To overcome this challenge, we propose a dynamic graph index named Vista to replace the rigid patterns and configurations of previous solutions. Our dynamic pattern generates edge candidates and selects graph edges based on vector distribution. Vista compensates for nodes with low  $k$ -NN connectivity, ensuring sufficient routing edges to identify them efficiently. It mitigates the cost of retrieving ground truth vectors with poor  $k$ -NN connectivity, significantly reducing the time cost in ANNS retrieval, especially for high-recall queries. Our main contributions can be summarized as follows:

**1. Identifying the challenge:** We find that for imbalanced datasets, the main bottleneck for ANNS is in the retrieval of vectors with low  $k$ -NN connectivity. This is particularly important for embedding vectors from emerging sequence-to-vector models such as LLMs and GNNs, and we provide evidence for this phenomena in Section III.

**2. Dynamic index design:** We design a dynamic ANNS index for constructing graph edges based on vector distribution to ensure good connectivity of all vectors across the dataset, thereby reducing search costs in ANNS tasks, especially for high-recall responses.

**3. Comprehensive evaluation:** We implement Vista efficiently with good parallelism for index construction and

retrieval. Our implementation is evaluated on public and real-world industry datasets, demonstrating its success in efficient ANNS queries and scalability in highly parallel environments.

## II. BACKGROUND AND RELATED WORK

### A. Problem Definition

In this paper, we focus on the  $k$  approximate nearest neighbor search task for high-dimensional vectors, aiming to discover the  $k$  nearest neighbors for a given query. Since retrieving the exact nearest neighbors is often inefficient, our goal is for the ANNS index to return as many correct neighbors as possible efficiently.

### B. Previous Studies

The skewness in high-dimensional vectors for ANNS tasks is observed in previous studies. M. Radovanović et al. [50], [51] discuss the frequency with which a point appears among the  $k$  nearest neighbors of other points in a dataset, confirming the common existence of points with very high  $k$ -occurrences that effectively represent ‘popular’ nearest neighbors across various datasets. They also point out that such ‘popular’ points can frequently be included in the result list during the information retrieval process. Brankica Bratić et al. [11] examine the vector distribution for the NN-descent algorithm [19] and demonstrate that points with high in-degree in a  $k$ -NN graph result in better search quality in the NN-descent index. Although the imbalance distribution of vectors has been discussed and applied to various machine learning tasks [20], advanced ANNS graph indexes are not optimized for this problem. According to the recent evaluation results on ANNS graph indexes, the following are among the most efficient solutions for ANNS in large-scale scenarios:

NSG [22] and NSSG [21] propose monotonic search networks to ensure efficient retrieval while reducing index size. HNSW [40], [41] incorporates the small-world graph [31] with the relative neighborhood graph [28] to construct a sparse hierarchical index for retrieval. HVS [39] proposes a hierarchical quantization structure for efficiently locating query neighborhoods to improve efficiency. Vamana [29] introduces a distance factor for constructing long edges on a randomly initialized graph. HCNG [44] employs random partitions on feature space and constructs a minimum spanning tree in each partition. LSHAPG [64] combines hashing functions with a graph index to improve index construction efficiency and generate high-quality entry points for retrieval.  $\tau$ -MNG [45] optimizes the edge pruning strategy to lower search time complexity when the query and its nearest neighbors are close enough. ParlayANN [17], [42] introduces an optimized parallelism strategy for the efficient implementation of various types of ANNS indexes in high-parallelism scenarios.

## III. CHALLENGE AND MOTIVATION

With emerging vector datasets becoming more imbalanced, understanding their impact on the structure and performance of graph-based ANNS indexes is crucial. This section discusses and examines how dataset distribution affects these indexes, with notations summarized in Table II.

Notation	Definition
$m$	Upper bound of neighbor candidates
$n$	Upper bound of out-edges
$ \mathcal{X} $	The number of elements in set $\mathcal{X}$
$\mathcal{N}(v_i, k)$	Set of $k$ nearest neighbors of $v_i$
$\mathcal{M}(v_i, k)$	Set of vectors for which $v_i$ is among the $k$ nearest neighbors
$\mathcal{I}(v_i)$	Set of in-edges for $v_i$ in proximity graph
$\mathcal{S}(v_i, \mathcal{X})$	Result of edge selection from $v_i$ to vectors in the set $\mathcal{X}$
$\mathcal{P}(v_i, k, \mathcal{X})$	Pruning result with a set of vectors selected from $\mathcal{X}$ , where $v_i$ is among the $k$ shortest outgoing edges from $v_j \in \mathcal{X}$
$\mathcal{R}(v_i, v_j, \mathcal{X})$	The rank of the distance between $v_i$ and $v_j$ among the distances from vectors in $\mathcal{X}$ to $v_i$ , ordered from smallest to largest

TABLE II: Summary of notations.

### A. Analysis on Graph Index and Imbalanced Distribution

To facilitate this analysis, Table III summarizes the construction process of advanced graph-based indexes, emphasizing the impact of dataset distribution. A recent benchmark [61] identifies five key components: initialization, edge candidate acquisition, edge selection, seed preprocessing, and connectivity assurance. We focus on the two most critical components influenced by vector distribution: edge candidate acquisition and edge selection.

For all graph indexes, edge candidate acquisition involves generating a subset of vectors close to each database vector  $v$  as potential linking candidates. Strategies vary across algorithms: many, including HNSW [41], NSG [22], and Vamana [29], use  $v$  as a query vector on the initialized index, retaining the closest vectors (HNSW, NSG) or all visited nodes (Vamana). HCNG [44] partitions the dataset, treating vectors in the same partition as candidates. Edges are then selected using distance-based pruning rules, such as the relative neighborhood graph (RNG) in HNSW and Vamana, monotonic RNG in NSG, and minimum spanning tree (MST) in HCNG. Some indexes, like HNSW and Vamana, also add reverse edges to ensure bi-directional connections, subject to an out-degree limit.

From the discussed edge construction process, in-edges for a vector  $v_i$  come from two sources: (1) reverse edges from its selected edge neighbors and (2) out-edges from vectors that select  $v_i$  as a neighbor based on edge selection strategies.

The first type of edges is represented by  $\mathcal{S}(v_i, \mathcal{N}(v_i, m))$ , indicating reverse edges from neighbors of vector  $v_i$  based on a specific edge selection strategy. The second type is represented by  $v_j \mid v_i \in \mathcal{S}(v_j, \mathcal{N}(v_j, m))$ , denoting vectors  $v_j$  that select  $v_i$  as a neighbor, making  $v_i$  an edge candidate. The final set of in-edges is the union of these two sets, clipped to the upper bound of  $n$  out-edges. i.e.

$$\begin{aligned} \mathcal{I}(v_i) = & \mathcal{P}(v_i, n, (\mathcal{S}(v_i, \mathcal{N}(v_i, m)))) \\ & \cup \mathcal{P}(v_i, n, \{v_j \mid v_i \in \mathcal{S}(v_j, \mathcal{N}(v_j, m))\}) \end{aligned} \quad (1)$$

From Equation 1, the number of in-edges for a vector is primarily affected by how many vectors consider it as a neighbor. This depends on: (1) the pruning process for both edge types, denoted as  $\mathcal{P}(v_i, n, \mathcal{X})$ , requiring  $v_i$  to be an  $n$ -closest edge candidate for vectors within  $\mathcal{X}$ , and (2) the number of vectors that select  $v_i$  as a neighbor, impacting the second type of edges. In the absence of edge pruning

Graph Index	Year	Initialization	Edge Candidate Acquisition	Candidate Size Control	Edge Selection Strategy	Edge Size Control
HNSW [41]	2018	Random Seed and Incremental Insertion	Search	Fixed Bound	Relative Neighborhood Graph (RNG)	Fixed bound
Vamana [29]	2019	Random Regularized Graph	Search	All Visited Nodes	RNG and Distance Parameter	Fixed Bound
HCNNG [44]	2019	Random Partition Trees	Vector Pairs in Partitions	Fixed Bound	Minimum Spanning Tree	Fixed Bound
NSSG [21]	2021	$k$ -NN Graph	Search	Fixed Bound	Monotonic Network and Angle Parameter	Fixed Bound
LSHAPG [64]	2023	LSH Partition	Search	Fixed Bound	$k$ -NN Graph	Fixed Bound
Vista	2024	Random Partition Trees and Approximate $k$ -NN Graph	Optimized Search	Dynamic Bound based on Distribution	RNG	Dynamic Edge Exchange

TABLE III: Index construction flow of advanced graph-based methods. Vista employs a dynamic index pattern tailored to vector distribution to address vector skewness.

( $\mathcal{S}(v, \mathcal{X}) = \mathcal{X}$ ), the index becomes a bi-directional  $k$ -NN graph. For each vector  $v_i$ , bi-directional edges are formed with  $\mathcal{N}(v_i, m) \cup \mathcal{M}(v_i, m)$ , leading to the in-degree of vector  $v_i$ :

$$\begin{aligned} \mathcal{I}(v_i) &= \{v_j \in \mathcal{N}(v_i, m) \cup \mathcal{M}(v_i, m) \mid \\ &\quad \mathcal{R}(v_j, v_i, \mathcal{N}(v_j, m) \cup \mathcal{M}(v_j, m)) \leq n\} \end{aligned} \quad (2)$$

As indicated by Equation 2, this pattern results in an imbalance in vector connectivity when the vector distribution is skewed. For vector  $v_i$ , if  $|\mathcal{M}(v_i, m)|$  is small or zero, few or no vectors will attempt to connect to it. Moreover, the reverse edge from  $v_j \in \mathcal{N}(v_i, m)$  may be pruned in favor of shorter edges in  $\mathcal{N}(v_j, m) \cup \mathcal{M}(v_j, m)$  due to the upper bound  $n$ , leading to poor connectivity for  $v_i$ . Such imbalances in vector distribution are commonly observed in high-dimensional datasets, as noted in several studies [11], [50], [51]. To guarantee at least one in-edge for each vector, the minimum upper bound on the out-degree across the entire dataset is:

$$n_{min} = \max_{v_i \in \mathcal{V}} \min_{v_j \in \mathcal{N}(v_i, m) \cup \mathcal{M}(v_i, m)} (\mathcal{R}(v_j, v_i, \mathcal{N}(v_j, m) \cup \mathcal{M}(v_j, m))) \quad (3)$$

In imbalanced datasets, Equation 3 highlights a potential conflict between maintaining vector connectivity and enforcing a fixed upper bound on out-degrees. Isolated points like  $v_i$ , which are far from all neighbors  $v_j$ , require many edges to connect vectors between  $v_j$  and  $\mathcal{N}(v_j, m) \cup \mathcal{M}(v_j, m)$  when their distances are smaller than the large distance between  $v_i$  and  $v_j$ . This necessitates a large out-degree bound to maintain  $v_i$ 's connectivity. Variants of bi-directional  $k$ -NN graphs with specific edge selection strategies encounter similar connectivity challenges due to fixed out-degree limits.

In high-dimensional, large-scale datasets, maintaining strict out-degree limits while ensuring connectivity is often impractical due to computational constraints, with typical bounds set to tens. To guarantee a search path to all vectors, some indexes, like NSG [22], add edges to vectors lacking in-edges. However, this can exceed the predefined out-degree limit, leading to unavoidable hubs—vectors with a disproportionately large number of out-edges.

### B. Evaluation on the Impact of Imbalanced Distribution

In this work, we refer to the **in-degree of a vector in a  $k$ -NN graph**, i.e.  $|\mathcal{M}(v_i, k)|$ , as its ' $k$ -NN connectivity' to this particular in-degree from that of other graphs present in the workflow. To assess the impact of vector imbalance on index structure and performance, we conducted preliminary experiments on three ANNS datasets: SIFT, DEEP, and ByteECom1, each consisting of 1 million vectors, using the Vamana [29] graph index. The maximum number of edges and the size of the search list during index construction were both set to 50. As we will show,  $k$ -NN connectivity is an important proxy for performance slowdown.

**Distribution of  $k$ -NN Connectivity.** First, we explore the distribution of  $k$ -NN connectivity on ANNS datasets. In this experiment, we set  $k$  equal to 50. The histogram of 50-NN connectivity distribution is shown in Figure 3. From the results, we observe that the  $k$ -NN connectivity follows a long-tail imbalanced distribution. Specifically, many vectors have relatively low  $k$ -NN connectivity. For instance, in all datasets, the connectivity of about 40% points is under 30, while about 10 percent of points are well connected, with an in-degree higher than 100 in the  $k$ -NN graph. Comparing the three datasets, the ByteECom1 dataset contains more vectors with an in-degree below 50, whereas the SIFT and DEEP datasets have more vectors with  $k$ -NN connectivity over 100.

**Impact of  $k$ -NN Connectivity on Index Structure.** Next, we examine how such an imbalance in  $k$ -NN connectivity affects the edge structure of the graph index. We analyze the number of in-edges from its 50 nearest neighbors in the constructed Vamana graph concerning the  $k$ -NN connectivity of points. The long edges are not included as they are mainly used for navigating to different regions of the whole index, and the search process from the neighborhood of the query takes the majority of search time [34]. The examination results are shown in Figure 4 with scatters. For clear visualization, each scatter point represents the centroid of 1000 nearby points.

In all datasets, the number of in-edges from the 50 nearest neighbors increases with the  $k$ -NN connectivity. This supports our analysis of graph index construction: vectors with higher  $k$ -NN connectivity tend to receive more links from their neighbors, as described by Equation 1. Based on this observation, we expect that well-connected vectors will be more easily retrieved from their neighboring vectors, whereas vectors with

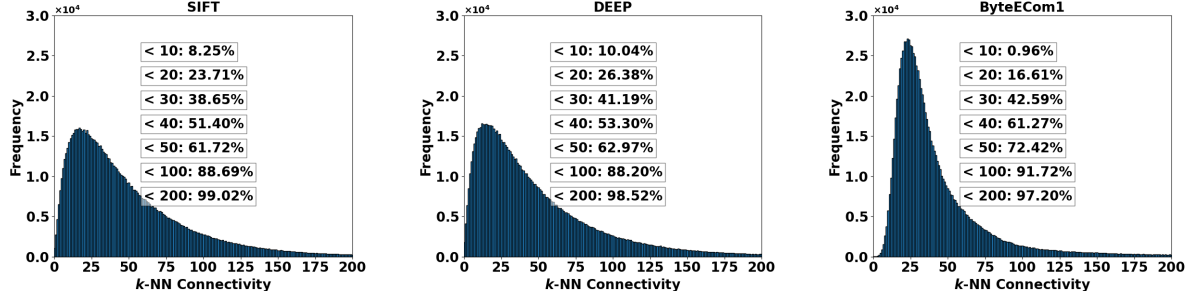


Fig. 3:  $k$ -NN connectivity distribution in a 50-NN graph on ANNS datasets.  $k$ -NN connectivity for each point indicates the number of vectors that consider it an edge candidate. The percentages of points with  $k$ -NN connectivity lower than certain bounds are plotted in the figure. We observe the distribution of  $k$ -NN connectivity is imbalanced in all datasets.

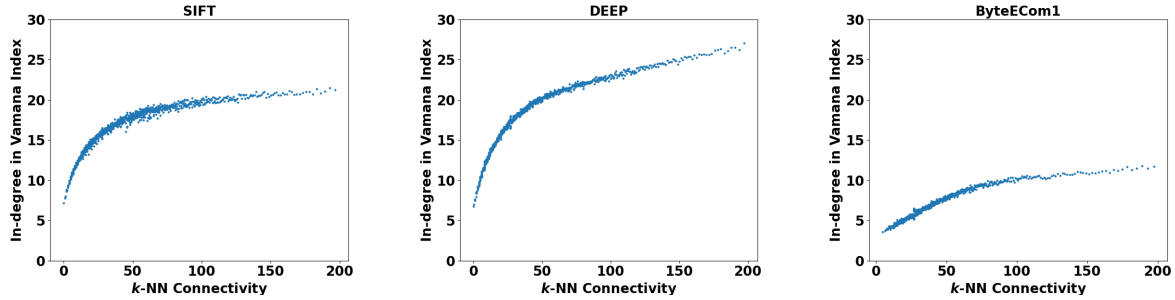


Fig. 4: In-degree from 50 nearest neighbors in Vamana graph with respect to the  $k$ -NN connectivity of points. We observe an increment in the number of in-edges from neighbors in Vamana with the  $k$ -NN connectivity of points.

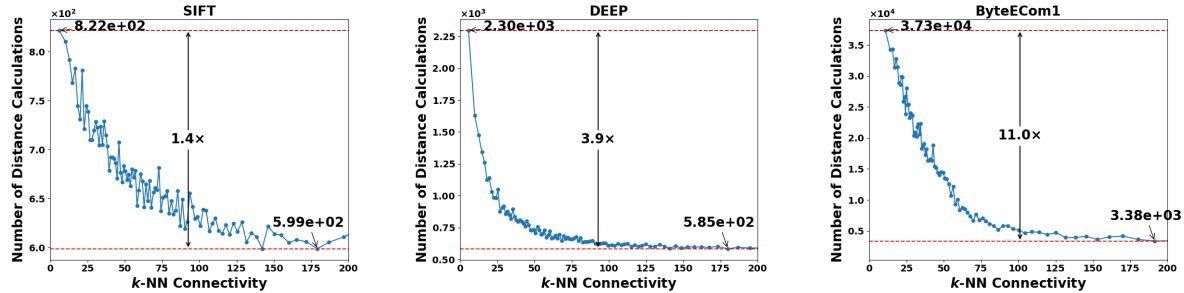


Fig. 5: Minimum number of distance calculations for searching ground truth vectors with respect to their  $k$ -NN connectivity. Vectors with higher  $k$ -NN connectivity are easier to find, while those with lower connectivity are more difficult to retrieve.

poor connectivity will be harder to retrieve, which aligns with previous findings [11], [50].

**Impact of  $k$ -NN Connectivity on Search Efficiency.** We further explore the search cost of vectors by launching retrieval tasks with 10,000 query vectors and testing the minimum search cost for identifying ground truth vectors. In Figure 5, we report the minimum number of distance calculations required to find the ground truth vector as an indicator of search cost. The ratio between the highest and lowest search costs is plotted in the figure. Across the three evaluated datasets, the search cost for vectors continually decreases with  $k$ -NN connectivity due to more in-edges from their neighbors, as we analyzed. Vectors in ByteECOM1 demonstrate an impressive difference, with an 11-fold variation in search cost. Therefore,

we confirm that vectors with low  $k$ -NN connectivity are much more expensive to retrieve than other points.

Importantly, besides achieving high recall necessitating the search for vectors with low  $k$ -NN connectivity, which is inherently expensive as shown in previous figures, it also increases the cost of retrieving vectors with high  $k$ -NN connectivity. This is because searching for poorly connected vectors requires a large search list size, which is global for all queries. Consequently, the cost of retrieving well-connected vectors also rises. In Figure 6, we present the comparison of ground truth distribution and search cost between different recall performances. With higher recall performance at 0.95, more vectors with low  $k$ -NN connectivity need to be searched, as indicated by the gap between green and orange lines. Here,

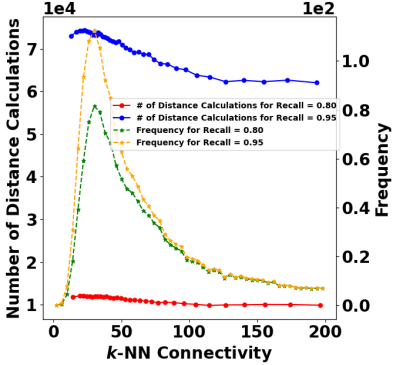


Fig. 6: Comparison of the distribution of retrieved ground truth vectors and search cost at different Recall10@10 (defined in Section V) on the ByteECom1 dataset. The result shows that achieving high recall performance requires searching for more vectors with low  $k$ -NN connectivity. This increased search effort for hard-to-retrieve vectors also raises the cost of searching vectors with high  $k$ -NN connectivity, due to the global configuration of search list size.

we observe a clear increase in the frequency of retrieved vectors with low  $k$ -NN connectivity (e.g., smaller than 50). Meanwhile, the search cost, represented by the number of distance calculations, increases for all vectors. Even though we can search well-connected vectors with relatively low computation costs, as shown by the red curve, the demand for retrieving hard-to-retrieve vectors with low  $k$ -NN connectivity increases the overall search cost by over sixfold due to the larger search list size in beam search, as shown by the blue curve. Thus, searching for points with low  $k$ -NN connectivity is the primary bottleneck in efficiency.

From our discussion and evaluation in this section, we complete the analysis of the impact of vector distribution, represented by  $k$ -NN connectivity, on graph index structure (Figure 4) and search efficiency (Figure 5 and Figure 6). It is observed that vectors with a lower in-degree in the  $k$ -NN graph, i.e., lower  $k$ -NN connectivity, tend to have a smaller in-degree in the constructed index from their neighbors, making them more difficult to identify as ground truth in retrieval. Additionally, new emerging datasets, such as those generated by models on text and graph data like ByteECom1, are more skewed than others and are more likely to suffer from these challenges. This makes the problem more pronounced in modern and future applications.

#### IV. INDEX DESIGN

Most advanced graph-based indexes use rigid patterns and configurations for all vectors during edge candidate generation and edge selection, disregarding the varying nature of vector distributions, as shown in Table III. However, as discussed in Section III, maintaining a fixed upper bound while ensuring vector connectivity often leads to conflicts, and vectors with low  $k$ -NN connectivity are significantly harder to retrieve due to fewer in-edges from their neighbors. Therefore, optimizing the graph index construction process specifically for hard-

---

#### Algorithm 1 Vista Index Construction Algorithm

---

```

Input: Dataset  $\mathcal{V}$ , Max leaf size in RPT  $L$ , Number of RPTs  $R$ , Number of nearest neighbors in initialization  $K$ 
Output: Constructed Graph Index  $Edges$ 
1: 1. Initialization
2:  $RPTs \leftarrow \text{CONSTRUCT-RPT}(\mathcal{V}, L, R)$ 
3:  $InEdges, OutEdges \leftarrow \text{INITIALIZE-NN}(\mathcal{V}, K, RPTs)$ 
4: 2. Edge Candidate Acquisition & Edge Selection
5: Get  $\alpha$  with Equation 5
6: Get one random projection tree:  $RPT \leftarrow RPTs[0]$ 
7: for  $v_i$  in  $\mathcal{V}$  do
8:   Get  $C_i$  with Equation 4
9:    $Candidates \leftarrow \text{BEAM-SEARCH}(v_i, RPT, InEdges, OutEdges, C_i, K, \alpha)$ 
10:   $InEdges, OutEdges \leftarrow \text{UPDATE-EDGE}(v_i, Candidates, InEdges, OutEdges, K)$ 
11: end for
12: for  $v_i$  in  $\mathcal{V}$  do
13:    $Edges[v_i] \leftarrow InEdges[v_i] \cup OutEdges[v_i]$ 
14: end for
15: 3. Dynamic Edge Exchange
16: for  $v_i$  in  $\mathcal{V}$  do
17:   if  $|Edges[v_i]| > K$  then
18:      $Edges \leftarrow \text{EXCHANGE-EDGE}(v_i, Edges)$ 
19:   end if
20: end for

```

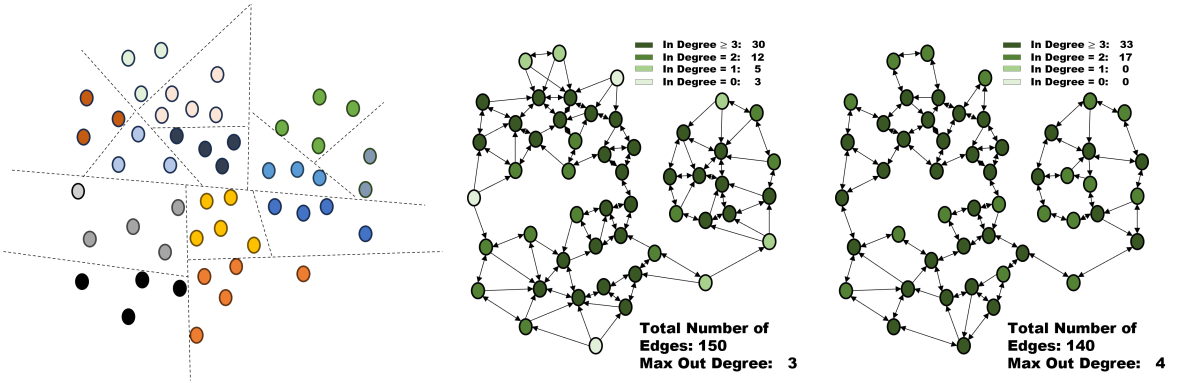
---

to-retrieve vectors with a distribution-aware approach could be highly beneficial. In this section, we introduce our dynamic index design, Vista, based on the distribution of  $k$ -NN connectivity. Vista aims to construct more edges for hard-to-retrieve vectors that likely have a low in-degree in traditional edge construction patterns. The core idea can be summarized as follows: 1. Generate more neighbor candidates to build edges to points with low  $k$ -NN connectivity. 2. Prevent the deletion of necessary edges linked to vectors with low  $k$ -NN connectivity.

#### A. Algorithm Description

The entire index construction flow of our design is summarized in Algorithm 1. Our dynamic index construction starts with an estimation process that captures the  $k$ -NN connectivity distribution of database vectors. As we aim to create efficient indexes for large-scale datasets, such as those exceeding 100 million vectors, calculating the accurate  $k$ -NN relationship to compute connectivity for large-scale vectors is prohibitively expensive. Instead, we employ an approximation process to estimate the  $k$ -NN structure efficiently.

**Initialization and Beam Search (Algorithm 2, 3, 4):** We first construct multiple random projection trees (RPTs) [15] to partition the original dataset into disjoint subspaces with hyperplanes, as described in Algorithm 2, with control on the maximum size of each partition. All vectors within the same partition are potential  $k$ -NN neighbors to each other, so we calculate the distances between them and preserve the  $K$  closest neighbors for all vectors as approximate results. With a sufficient number of RPTs (e.g., 64), we discover  $K$  approximate neighbors for all vectors as an initialization of our graph index, as outlined in Algorithm 3. Additionally, we keep one random projection tree for further index construction and retrieval using the beam search algorithm, as described in Algorithm 4. The space partition result of the RPT provides



(a) Space partition with random partition tree. (b) Initialization with 3-NN graph. (c) Vista index construction result.

Fig. 7: An example of our index construction process in 2-dimensional space with 50 vectors. Figure (a): the feature space is partitioned into disjoint subspaces using RPT, with vectors in the same partition (indicated by the same color) considered as potential neighbors. Figure (b): the generated  $k$ -NN graph with  $k = 3$  for initialization, where points are color-coded based on their in-degree; darker colors indicate higher in-degree. Figure (c): the final index construction of Vista, where light-colored points with low in-degrees (e.g.,  $\leq 1$ ) are eliminated and the total number of edges is reduced from 150 to 140.

---

#### Algorithm 2 CONSTRUCT-RPT( $\mathcal{V}, L, R$ )

---

**Input:** Dataset  $\mathcal{V}$ , Max leaf size in RPT  $L$ , Number of RPTs  $R$   
**Output:** Constructed random projection trees  $RPTs$

- 1:  $RPTs \leftarrow \emptyset$
- 2: **for**  $i = 1, \dots, R$  **do**
- 3:      $RPTs \leftarrow RPTs \cup \text{RECURSIVE-PARTITION}(\mathcal{V})$
- 4: **end for**
- 5: **function** RECURSIVE-PARTITION( $\mathcal{X}$ )
- 6:     **if**  $|\mathcal{X}| < L$  **then**
- 7:         **return**  $[\mathcal{X}]$
- 8:     **end if**
- 9:     Randomly select two vectors  $v_1$  and  $v_2$  in  $\mathcal{X}$
- 10:    Split  $\mathcal{X}$  into two subsets  $\mathcal{X}_1$  and  $\mathcal{X}_2$ , where vectors are closer to  $v_1$  or  $v_2$  respectively
- 11:    **return**  $[\text{RECURSIVE-PARTITION}(\mathcal{X}_1), \text{RECURSIVE-PARTITION}(\mathcal{X}_2)]$
- 12: **end function**

---

a high-quality starting neighborhood for queries. For a given query vector, we first assign it to RPT space partitions and start the query process with the vector closest to the centroid of all vectors in the assigned partition. As vectors with low  $k$ -NN connectivity are hard to retrieve with out-edges, we maintain an additional structure that keeps the in-edges of all vectors.

An example of this process is presented in Figure 7 (a), where the vectors in different partitions are plotted with different colors. The distances between vectors of the same color are calculated, and we keep the  $K$  nearest neighbors for all vectors. Generating more RPTs helps improve the accuracy of the  $k$ -NN relationship. Figure 7 (b) provides an example of a 3-NN graph of our initialization result, colored by  $k$ -NN connectivity. There are many points with in-degrees less than 2, and some points have no in-edges at all, meaning they are never retrieved through the graph.

**Edge Candidate Acquisition (Algorithm 4):** We continue the edge candidate acquisition based on the constructed approximate  $k$ -NN graph. To generate edge candidates, we search each vector as a query to identify its close neighbors as candidates. To improve the quality of candidates, we retrieve

---

#### Algorithm 3 INITIALIZE-NN( $\mathcal{V}, K, RPTs$ )

---

**Input:** Dataset  $\mathcal{V}$ , Number of nearest neighbors in initialization  $K$ , Random projection trees  $RPTs$   
**Output:** Out-edges of vectors  $OutEdges$  and In-edges of vectors  $InEdges$

- 1: **for**  $v_i \in \mathcal{V}$  **do**
- 2:      $OutEdges[v_i] \leftarrow \emptyset$
- 3:      $InEdges[v_i] \leftarrow \emptyset$
- 4: **end for**
- 5: **for**  $i = 1, \dots, R$  **do**
- 6:     **for** each partition in  $i$ -th RPT **do**
- 7:         **for** each vector pair  $(v_i, v_j)$  in the partition **do**
- 8:             Update  $OutEdges[v_i]$  with  $v_j$ , keep at most  $K$  closest vectors
- 9:             Update  $OutEdges[v_j]$  with  $v_i$ , keep at most  $K$  closest vectors
- 10:         **end for**
- 11:     **end for**
- 12: **end for**
- 13: **for**  $v_i \in \mathcal{V}$  **do**
- 14:     **for**  $v_j \in OutEdges[v_i]$  **do**
- 15:          $InEdges[v_j] \leftarrow InEdges[v_j] \cup v_i$
- 16:     **end for**
- 17: **end for**

---

both out-edges and in-edges in the approximate  $k$ -NN graph. Our analysis of  $k$ -NN connectivity indicates that points with low  $k$ -NN connectivity have very few or even no in-edges in the initial index, making them very difficult, or even impossible, to retrieve if we only search the out-edges, thus we need to search the in-edges. Since the in-degree of vectors is not controlled and some points have a very large in-degree, we randomly sample  $K$  in-edges for retrieval if the number of in-edges exceeds  $K$ , in order to improve construction efficiency.

Moreover, most proposed graph indexes use a fixed bound for the number of candidates, while our analysis shows that vectors with low  $k$ -NN connectivity are more challenging to retrieve with traditional indexes. Thus, we assign a larger candidate budget for vectors with low in-degree in the approximate  $k$ -NN graph to balance the difficulty in retrieval. We use an automated approach to learn all distribution-related

---

**Algorithm 4** BEAM-SEARCH( $q, RPT, InEdges, OutEdges, C, K, \alpha$ )

**Input:** Query vector  $q$ , Random projection tree  $RPT$ , Out-edges of vectors  $OutEdges$  and In-edges of vectors  $InEdges$ , Size of search list  $C$ , Maximum number of in-edges to visit  $K$ , Parameter for calculating number of result neighbors  $\alpha$

**Output:**  $\mathcal{C}$  with  $\alpha \cdot C$  closest neighbors to  $q$

- 1: Assign  $q$  to space partitions in  $RPT$ , and  $v$  is the vector in the assigned partition closest to the centroid
- 2:  $\mathcal{L} \leftarrow v$
- 3:  $\mathcal{C} \leftarrow v$
- 4: **while**  $\mathcal{L}$  includes unexpanded point(s) **do**
- 5:    $p \leftarrow$  closest unexpanded node in  $\mathcal{L}$
- 6:   Mark  $p$  as expanded
- 7:   Update  $\mathcal{L}$  and  $\mathcal{C}$  with  $OutEdges[p]$
- 8:   Update  $\mathcal{L}$  and  $\mathcal{C}$  with at most  $K$  elements sampled from  $InEdges[p]$
- 9:   Keep at most  $C$  closest vectors to  $q$  in  $\mathcal{L}$
- 10:   Keep at most  $\alpha \cdot C$  closest vectors to  $q$  in  $\mathcal{C}$
- 11: **end while**

---

parameters, making Vista both user-friendly and optimized. The details of this parameter determination process are outlined below.

Given a vector  $v_i$  with  $k$ -NN connectivity  $p_i$  and the number of approximate nearest neighbors  $K$  used in initialization, its size of the search list in the beam search process is calculated as:

$$C_i = K + (K - \min(K, p_i)) \quad (4)$$

This function provides linear compensation for vectors with in-degrees below  $K$  in the approximate  $k$ -NN graph. Vectors with  $k$ -NN connectivity greater than  $K$  have a search list size set to  $K$ , while those with connectivity below  $K$  have it set to  $2 \cdot K - p_i > K$ , allowing them to construct more in-edges in the Vista index.

To generate a sufficient number of candidates for edge selection, we retain the closest  $\alpha \cdot C_i$  vectors as edge candidates. Here,  $\alpha$  is a parameter learned from the relative neighborhood graph (RNG) [7], [28] edge selection process for the given dataset. Starting with an approximate  $k$ -NN relationship containing  $K$  neighbors, we sample a small subset of the dataset (e.g., 1,000 vectors) and apply the RNG edge pruning algorithm to their  $K$  neighbors. If the average number of preserved edges per vector is  $P$ , then:

$$\alpha = K/P \quad (5)$$

By learning the distribution-specific parameter  $\alpha$ , we ensure an adequate number of edge candidates while maintaining efficiency and preventing excess.

**Edge Selection and Update (Algorithm 5):** With generated candidates for all vectors, we construct edges between each vector and its candidates using the RNG principle. Candidates are sorted by their distance to the vector, and selection starts from the closest. According to the RNG rule, a candidate is chosen only if it is closer to the base vector than any of the already selected candidates. Once all candidates are evaluated, we create edges from the selected candidates to the vector. Additionally, edges are formed from the vector to its selected candidates if the candidate is among the closest  $K$  edge candidates.

---

**Algorithm 5** UPDATE-EDGE( $v, Candidates, InEdges, OutEdges, K$ )

**Input:** Database vector  $v$ , Edge candidates  $Candidates$ , In-edges of vectors  $InEdges$ , Out-edges of vectors  $OutEdges$ , Upper bound of  $OutEdges$  size  $K$

**Output:** Updated in-edges  $InEdges$  and out-edges  $OutEdges$

- 1: Initialize selected candidates  $\mathcal{C} \leftarrow \emptyset$
- 2: **while**  $Candidates$  is not empty **do**
- 3:    $p \leftarrow$  closest vector in  $Candidates$  to  $v$
- 4:   Remove  $p$  from  $Candidates$
- 5:   **if**  $p$  is closer to  $v$  than any vectors in  $\mathcal{C}$  **then**
- 6:      $\mathcal{C} \leftarrow \mathcal{C} \cup \{p\}$
- 7:   **end if**
- 8: **end while**
- 9: **for**  $v_i \in OutEdges[v]$  **do**
- 10:   Remove  $v$  in  $InEdges[v_i]$
- 11: **end for**
- 12: **for**  $v_i \in \mathcal{C}$  **do**
- 13:    $InEdges[v_i] \leftarrow InEdges[v_i] \cup v$
- 14: **end for**
- 15:  $OutEdges[v] \leftarrow$  at most  $K$  closest elements to  $v$  in  $\mathcal{C}$

---

**Algorithm 6** DYNAMIC-EXCHANGE-EDGE( $v, Edges$ )

**Input:** Database vector  $v$ , Out-edges of vectors  $Edges$

**Output:** Updated out-edges of vectors  $Edges$

- 1: Initialize preserved edges  $\mathcal{C} \leftarrow \emptyset$
- 2: **while**  $Edges[v]$  is not empty **do**
- 3:    $p \leftarrow$  closest vector in  $Edges[v]$  to  $v$
- 4:   Remove  $p$  from  $Edges[v]$
- 5:    $ExchangeFlag \leftarrow$  False
- 6:   **for**  $s \in \mathcal{C}$  **do**
- 7:     **if**  $p$  is closer to  $s$  than  $v$  and  $|Edges[s]| < |\mathcal{C}| + |Edges[v]|$  **then**
- 8:        $Edges[s] \leftarrow Edges[s] \cup p$
- 9:        $ExchangeFlag \leftarrow$  True
- 10:      **break**
- 11:     **end if**
- 12:   **end for**
- 13:   **if**  $ExchangeFlag$  is False **then**
- 14:      $\mathcal{C} \leftarrow \mathcal{C} \cup p$
- 15:   **end if**
- 16: **end while**
- 17:  $Edges[v] \leftarrow \mathcal{C}$

---

Notably, there is no fixed upper bound for controlling the maximum number of final out-degrees in our edge selection process. The upper bound  $K$  applies only to the set  $OutEdges$ , while we maintain an independent set  $InEdges$ . The final edge structure is based on the union of these two sets (line 13 in Algorithm 1). There is no fixed bound for the  $InEdges$  set, and we expect vectors with low  $k$ -NN connectivity to acquire more in-edges from this set due to their larger candidate set size based on Equation 4.

**Dynamic Edge Exchange (Algorithm 6):** As pointed out in Equation 3, incorporating a fixed upper bound on the final out-degrees often conflicts with ensuring the connectivity of points, particularly for vectors with low  $k$ -NN connectivity. However, constructing edges without bound on the out-degree can lead to hubs, which are vectors with excessively large out-degrees within the graph index. These hubs can introduce unnecessary search costs due to expansions from them.

In Vista, we employ a dynamic edge exchange process based on vector distribution to mitigate the problem of hubness. After the edge selection process, we replace the out-edges of hub vectors with edges between their out-neighbors to reduce their out-degrees while maintaining the RNG condition, thereby en-

suring efficient routing properties. Specifically, we examine the out-edges of all vectors with out-degrees exceeding  $K$ . If an edge can be pruned by using an intermediate point with a lower out-degree, we replace the original out-edge with an edge from the intermediate point to the target. This approach helps to maintain efficiency while reducing unnecessary connectivity from hub nodes.

The main difference between our design and traditional edge pruning strategies with fixed bounds is that we do not directly delete the edges. Instead, we replace the edge with another one based on the RNG condition and out-degree distribution, a process we call edge exchange. This pattern protects the edges connected to poorly connected points, ensuring there are still sufficient edges linked to them after the exchange. We present an example of our index construction result in Figure 7 (c). Compared with the initialization result in Figure 7 (b), our index prunes the edges using the RNG rule to remove long edges, thus reducing the total number of edges and generating a sparse graph. We also ensure there are sufficient edges to points with low  $k$ -NN connectivity, reducing their retrieval cost by excluding points with low in-degrees from neighbors, e.g.,  $<= 1$ . Although our index does not control the maximum out-degree with a fixed bound, resulting in the maximum out-degree increasing from 3 to 4, our edge exchange pattern introduced in Algorithm 6 helps mitigate this problem.

### B. Complexity Analysis

Let  $N$  be the total number of vectors in the dataset. The search complexity of Vista is  $O(\log(N))$  and the construction complexity is  $O(\log(N))$ . Refer to [23] for detailed analysis.

## V. EXPERIMENTS

We present a comprehensive evaluation of Vista, comparing it with leading graph-based indexes for large-scale ANNS. Vista demonstrates efficient, high-quality retrieval with affordable construction costs across public, synthetic, and ByteDance industry datasets. We assess its scalability across varying dataset sizes, explore parameter settings for cost-efficiency trade-offs, and confirm its optimization for retrieving challenging vectors. These results highlight Vista’s performance and competitiveness in ANNS tasks. More evaluations and discussions is available in our technical report [23].

### A. Experimental Setting

**Datasets.** In our evaluation, we include datasets from five sources, varying in scale from 1 million to 1 billion vectors, as shown in Table IV. The DEEP dataset consists of embedding vectors from GoogleNet [55] for image classification. We conduct experiments on varying scales, ranging from 1 million to 1 billion vectors from the DEEP embeddings. The smaller-scale subsets are randomly sampled from the public 1 billion vector dataset. ByteECom1 and ByteECom2 are datasets used in ByteDance’s real-world e-commerce scenarios. These embedding vectors are generated from an e-commerce graph with billions of nodes and approximately 50 billion edges using the GNN algorithm LINE [56]. For the stress test on vector

skewness, we generate million-scale synthetic datasets with varying distributions. The Synthetic Uniform dataset contains 1 million vectors with dimensions uniformly distributed as  $U(-1, 1)$ . For Gaussian-distributed vectors, we generate 1 million vectors with 1 to 100 clusters, where ‘Synthetic A’ represents A clusters. Each cluster’s center is defined by its binary ID (e.g., cluster 1: [0, ..., 1], cluster 2: [0, ..., 1, 0]), with equal-sized clusters and data points following a Gaussian distribution (variance = 1.0) in each dimension.

All datasets in the evaluation employ 10,000 queries for retrieval, which are not included in the database vectors. We include the local intrinsic dimension (LID) [5] of the datasets as an indicator of the retrieval difficulty, where a higher LID indicates greater difficulty.

Name	Dimension	Size	LID	Distance	Feature
DEEP	96	1 million 10 million 100 million 1 billion	3.9	Euclidean	Image
ByteECom1	128	1 million 10 million 100 million 700 million	5.6	Cosine	Graph
ByteECom2	128	1 million 10 million 100 million	10.7	Cosine	Graph
Uniform	32	1 million	5.1	Euclidean	Uniform Distribution
Gaussian	32	1 million with number of clusters from 1 to 100	5.6	Euclidean	Gaussian Distribution

TABLE IV: Summary of Datasets in Evaluation

**Machine and Measurement.** All experimental indexing and evaluation tasks are conducted on a server equipped with an Intel(R) Xeon(R) Platinum 8336C CPU and 2TB of DRAM memory. This server features a total of 128 cores, all of which were utilized for both the construction and retrieval phases of our experiments using OpenMP for parallelism. This setup matches real-world application scenarios that require fast index construction and high throughput. The evaluation metrics employed in our study are as follows:

1. Construction Time: This metric measures the time consumption in seconds for constructing the ANNS index with a given parameter configuration.

2. Queries Per Second (QPS): This metric quantifies the throughput of the system, indicating the number of queries it can process per second.

3. Recall@10 for 10 Neighbors (Recall10@10): This metric measures the accuracy of the search, defined as the ratio of correctly identified nearest neighbors among the top 10 ground truth neighbors for queries.

**Baselines, Implementations, and Parameter Settings.** We benchmark Vista against leading graph-based indexes known for large-scale ANNS efficiency, including HNSW [41], HCNNG [44], Vamana [29], and LSHAPG [64], following guidelines from recent literature [9], [17], [62]. We carefully tune each baseline’s construction parameters based on their research papers and documentation. For all benchmarks, we use their most optimized public implementations on large-scale datasets. ParlayANN [3] is used for Vamana and HCNNG, while an earlier HNSW version [1] and the

original LSHAPG implementation [2] are used. We set the maximum edges to 128 and the search list size to 125 for HNSW and Vamana [29], configure HCNG with 30 clusters and 1000 partitions [17], [42], and use the original LSHAPG setup [64]. Vista maintains a consistent configuration across experiments, except for Section V-E, which covers variations. Configurations are summarized in Table V.

Index	Construction Parameter Settings
HNSW	$efConstruction = 125, m = 64$
Vamana	$R = 128, L = 125, \alpha = 1.2$
HCNG	$T = 50, L_s = 1000, s = 3$
LSHAPG	$K = 16, L = 2, T = 24, T' = 2T, p_\tau = 0.95$
Ours	$K = 50, R = 32, L = 100$

TABLE V: Summary of Index Configuration

### B. Evaluation on Search Performance

In this section, we report the search performance of all indexes based on Recall10@10 and QPS, excluding those unable to complete construction within 24 hours.

Achieving robust performance across datasets of varying sizes is critical for modern applications. We analyze all indexes, including our proposed Vista, using the DEEP, ByteECom1, and ByteECom2 datasets at scales from 1M to 1B vectors. The results, shown in Figure 8 and Table VI, highlight Vista’s performance across different scales. LSHAPG results are omitted where construction time exceeds 24 hours. We highlight ours Key observations below.

**Superior Performance:** Vista surpasses all baselines across the evaluated recall range on all datasets, confirming the efficiency of our index design and implementation. Among the evaluated baselines, Vamana is the second-best in efficiency and stability on average, followed by HCNG, HNSW, and LSHAPG. On DEEP-1B dataset, Vista is  $1.5\times$  faster than Vamana and  $1.9\times$  faster than HCNG at recall levels of 0.96 and 0.98. Additionally, Vista achieves  $2.0\times$  faster performance at 0.92 recall on the ByteECom1-100M dataset and  $6.1\times$  faster performance at 0.80 recall on the ByteECom1-700M dataset. These results confirm the success of our index design in improving retrieval performance.

**Improvement with Recall:** The performance curve supports our statement regarding performance improvement with increasing recall. Across all evaluated real-world datasets of different scales, Vista consistently outperforms the baselines in terms of QPS, with a larger or at least comparable gap at higher recall levels. For example, on the ByteECom1-100M dataset, acceleration improves from 1.4 to 2.0 for Vamana as the required recall increases from 0.88 to 0.92. On the ByteECom1-700M dataset, the acceleration over HCNG increases from 2.3 to 8.5 as the required recall rises from 0.80 to 0.88. On the ByteECom2-10M dataset, the acceleration over Vamana increases from 1.5 to 3.4 as the required recall rises from 0.70 to 0.90. On DEEP datasets, the acceleration remains stable. This improvement is due to our optimization for hard-to-retrieve points with low  $k$ -NN connectivity. At higher recall levels, more challenging vectors need to be retrieved, causing baseline approaches to spend significantly more time searching

for these points compared to Vista. These results confirm the effectiveness of Vista in handling points with low  $k$ -NN connectivity, thereby improving efficiency in high-recall.

**Improvement with Scale:** In addition to Vista’s superior efficiency across all evaluated scales, we observe greater or comparable improvements as the dataset size increases, particularly for industry datasets. This indicates that Vista maintains or even enhances its efficiency on larger datasets for the same recall performance. For instance, compared to Vamana on ByteECom1, Vista achieves a  $2.7\times$  acceleration at a recall of 0.96 for 10 million vectors, compared to  $1.5\times$  for 1 million vectors. On ByteECom2, the acceleration at 0.90 recall is  $3.4\times$  for 10 million vectors, surpassing the  $1.1\times$  acceleration at the same recall for 1 million vectors.

Similarly, Vista shows even greater improvements over HCNG on larger datasets. For instance, at 0.92 recall on ByteECom1 with 100 million vectors, Vista achieves a  $4.1\times$  acceleration, compared to  $1.6\times$  for 10 million vectors. For 700 million vectors at 0.88 recall, the acceleration reaches  $8.5\times$ , significantly higher than the  $3.8\times$  observed for 100 million vectors. On ByteECom2, Vista achieves  $9.4\times$  acceleration at 0.70 recall for 100 million vectors, compared to  $2.0\times$  for 10 million vectors. At 0.90 recall, acceleration is  $3.4\times$  for 10 million vectors and  $1.3\times$  for 1 million vectors. These results suggest that larger datasets impose higher retrieval costs for imbalanced vectors with the same edge configuration, while smaller datasets allow vectors to cover a larger local space, including more vectors with low  $k$ -NN connectivity. This evaluation underscores Vista’s scalability and efficiency in managing large-scale datasets.

On the DEEP datasets, the improvement remains relatively stable with increasing scale and recall. This may be attributed to the dataset’s inherent ease (as indicated by its lower Local Intrinsic Dimensionality), resulting in fewer hard-to-retrieve vectors as scale and recall demands increase. Consequently, there is no clear trend of improvement across different settings. We also notice that GNN embedding datasets like ByteECom2, which have high LID, remain challenging even for state-of-the-art indexes, indicating that modern application datasets with indistinguishable high-dimensional vectors still require more effective solutions.

### C. Evaluation on Vector Distribution

To demonstrate the performance of Vista on various distributions, we evaluate Vista and baseline methods on synthetic datasets. The search performance of Vista and four advanced baselines is shown in Figure 8, with Vista’s acceleration over the baselines detailed in Table VI. The results reveal several key observations: First, Vista consistently outperforms all baselines, showing significant acceleration, particularly at high recall levels (i.e.,  $> 0.90$ ). HCNG emerges as the second-best approach, with Vista achieving acceleration between  $1.1\times$  and  $2.6\times$  across recall levels and datasets. For other baselines, Vista’s acceleration is often higher, reaching tens of times. This demonstrates Vista’s efficiency and robustness across datasets with diverse distributions.

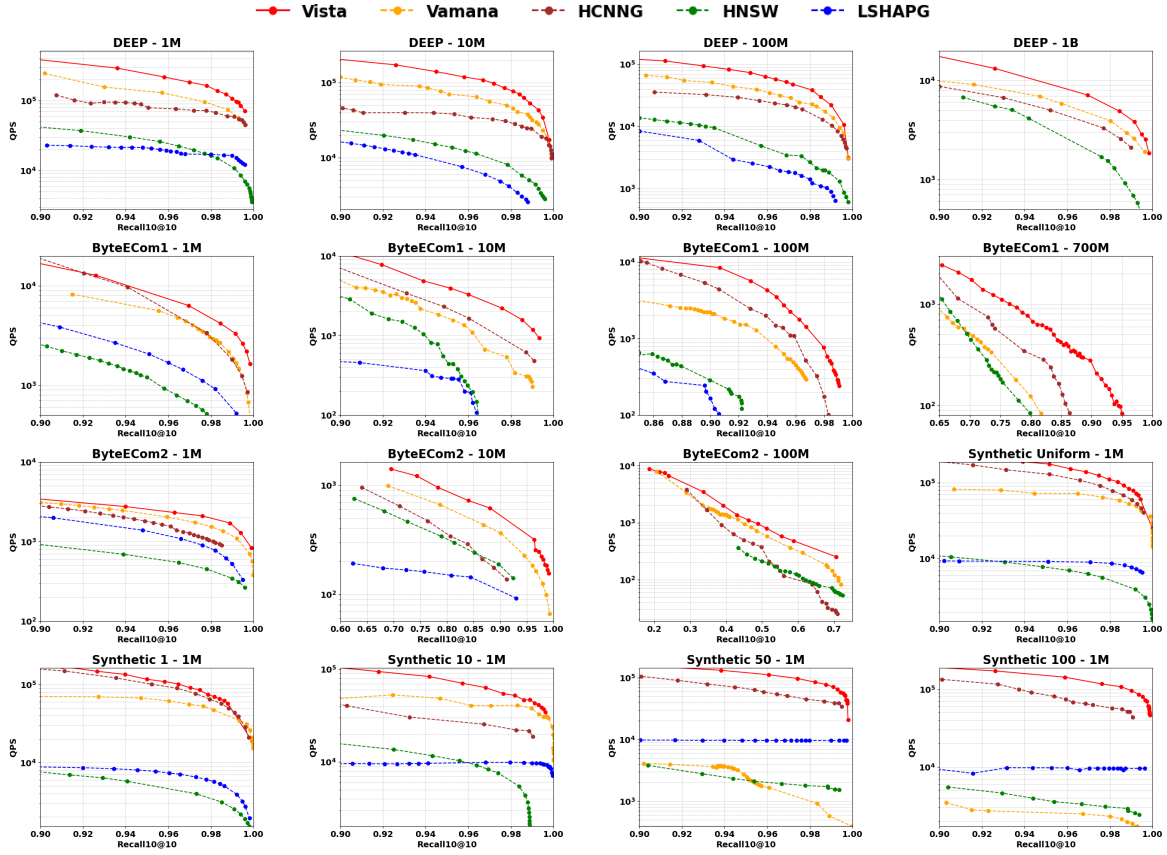


Fig. 8: Search performance with QPS-Recall curve on datasets in different scales.

In terms of dataset comparison, baseline indexes achieve the highest efficiency on the Synthetic Uniform dataset, followed by the Synthetic 1 dataset with a single Gaussian cluster. Their performance declines with increasing clusters (e.g., 50 or 100), indicating the challenges posed by multiple local clusters. In contrast, Vista maintains consistent search speed across datasets, demonstrating its robustness in handling multi-cluster distributions. As the number of clusters increases, Vista's acceleration over baselines becomes more pronounced, peaking at 50 or 100 clusters. This confirms Vista's effectiveness in handling complex ANNS tasks with local clusters, a crucial feature for sequence-based models, as discussed in Section I.

#### D. Evaluation on Construction Time

Here we report the construction time of all indexes over real-world datasets mentioned in the previous sections. The construction time is shown as a histogram in Figure 9. From the results, Vamana and HCNNG are the best-performing indexes across various datasets due to their effective algorithm design and efficient implementation in the ParlayANN library. Vista reports comparable construction time costs to Vamana and HCNNG, especially on datasets with scales up to hundreds of millions or billion. HNSW and LSHAPG are the least efficient solutions for all datasets due to their inefficient implementation in high-parallelism scenarios.

#### E. Discussion on Construction Parameters in Vista

Here we evaluate Vista's construction and search performance on the ByteECom2 dataset with 1 million vectors, focusing on the parameter  $K$ . Evaluation and discussion on RPT parameters, i.e.,  $R$  and  $L$ , can be found in our technical report [23]. Our default setting is  $K = 50$ . We vary  $K$  and report the retrieval and construction results in Figure 10.

From the results with varying  $K$ , increasing  $K$  initially improves search performance in the high recall range, with a slight decrease in performance for the low recall range. Since industrial applications typically require high recall, using a larger  $K$  setting is generally recommended. However, the trade-off for larger  $K$  lies in increased time and memory costs, as the index construction requires more time and larger memory due to the increased number of graph edges.

#### F. Optimization for Vectors with Low $k$ -NN Connectivity

To reveal the optimization results of Vista on vectors with low  $k$ -NN connectivity, we examine the search cost, indicated by the number of distance calculations, for vectors with different  $k$ -NN connectivity on Vista and the second-best baseline, Vamana, across two datasets, DEEP and ByteECom1, each with 1 million vectors. The results, shown in Figure 11, report the minimum number of distance calculations required to retrieve ground truth vectors and the ratio of search costs between the highest-cost vectors of the two methods. Vista

Index	DEEP-1M		DEEP-10M		DEEP-100M		DEEP-1B	
	Recall=0.96	Recall=0.98	Recall=0.96	Recall=0.98	Recall=0.96	Recall=0.98	Recall=0.96	Recall=0.98
Vamana	124491 (1.7x)	90060 (1.6x)	66529 (1.8x)	46833 (1.6x)	35545 (1.9x)	22995 (1.7x)	5628 (1.5x)	3943 (1.5x)
HCNNG	76898 (2.8x)	69726 (2.1x)	35044 (3.3x)	29258 (2.6x)	24785 (2.7x)	16656 (2.4x)	4477 (1.9x)	3037 (1.9x)
HNSW	24313 (8.9x)	16230 (9.0x)	12042 (9.7x)	7522 (10.2x)	4534 (14.7x)	2658 (15.0x)	2847 (3.0x)	1466 (3.9x)
LSHAPG	21301 (10.2x)	19320 (7.5x)	7108 (16.5x)	3973 (19.4x)	2789 (23.9x)	1420 (28.1x)	/	/
Vista	216211	145858	117289	77008	66544	39950	8617	5787
ByteECom1-1M	ByteECom1-10M		ByteECom1-100M		ByteECom1-700M		ByteECom1-1000M	
Vamana	Recall=0.96	Recall=0.98	Recall=0.92	Recall=0.96	Recall=0.88	Recall=0.92	Recall=0.80	Recall=0.88
HCNNG	5189 (1.5x)	3020 (1.6x)	3557 (2.2x)	1229 (2.7x)	6716 (1.4x)	3171 (2.0x)	123 (6.1x)	< 80
HNSW	887 (8.9x)	462 (10.8x)	1701 (4.5x)	229 (14.3x)	434 (22.2x)	176 (36.0x)	82 (9.1x)	< 80
LSHAPG	1686 (4.7x)	985 (5.0x)	424 (18.1x)	195 (16.8x)	262 (36.8x)	26 (243.3x)	/	/
Vista	7905	4974	7664	3285	9652	6326	749	327
ByteECom2-1M	ByteECom2-10M		ByteECom2-100M		Synthetic Uniform-1M		Synthetic Uniform-10M	
Vamana	Recall=0.90	Recall=0.98	Recall=0.70	Recall=0.90	Recall=0.60	Recall=0.70	Recall=0.96	Recall=0.98
HCNNG	3098 (1.1x)	1536 (1.2x)	950 (1.5x)	366 (1.5x)	321 (1.5x)	128 (2.2x)	71968 (2.2x)	61657 (1.8x)
HNSW	927 (3.8x)	435 (4.3x)	531 (2.6x)	184 (2.9x)	121 (3.9x)	65 (4.2x)	116050 (1.3x)	80812 (1.4x)
LSHAPG	2071 (1.7x)	819 (2.3x)	171 (8.1x)	110 (4.8x)	/	/	9099 (17.0x)	8682 (12.6x)
Vista	3542	1857	1388	532	472	276	154750	109290
Synthetic 1-M	Synthetic 10-M		Synthetic 50-M		Synthetic 100-M		Synthetic 1000-M	
Vamana	Recall=0.96	Recall=0.98	Recall=0.96	Recall=0.98	Recall=0.96	Recall=0.98	Recall=0.96	Recall=0.98
HCNNG	62008 (1.7x)	49133 (1.5x)	41392 (1.7x)	40833 (1.3x)	1671 (67.2x)	1032 (85.8x)	2516 (56.2x)	2307 (49.1x)
HNSW	94177 (1.1x)	64537 (1.3x)	26630 (2.6x)	22753 (2.3x)	57408 (2.0x)	44272 (2.0x)	73051 (1.9x)	57766 (2.0x)
LSHAPG	7350 (14.7x)	5829 (12.5x)	9928 (7.0x)	9922 (5.4x)	9648 (11.6x)	9636 (9.2x)	9670 (14.6x)	9583 (11.8x)
Vista	107807	72618	68894	53099	112362	88507	141521	113193

TABLE VI: QPS performance of various indexes across different datasets and recall thresholds. Acceleration of Vista is highlighted in red.

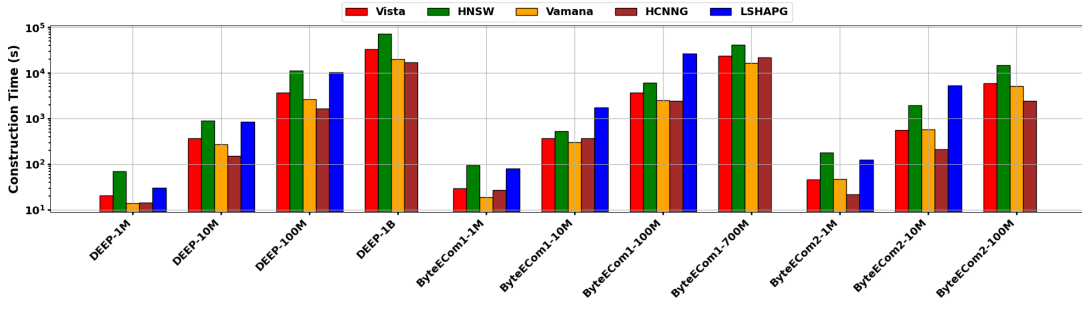


Fig. 9: Construction Time on Real-World Datasets.

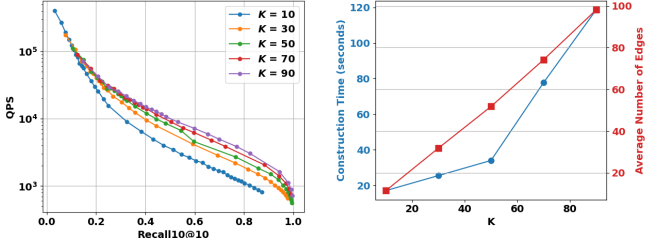


Fig. 10: Comparison on construction parameter setting on  $K$ . demonstrates a clear reduction in the cost of retrieving vectors with low  $k$ -NN connectivity, with search costs reduced by 2.1 and 2.2 times on two datasets, confirming its effectiveness in managing these vectors. This results in a slight increase in search cost for vectors with high  $k$ -NN connectivity. Since the cost of retrieving vectors with low  $k$ -NN connectivity is the bottleneck in ANNS systems (as indicated in Section III), Vista benefits from this trade-off.

## VI. CONCLUSION

We introduce Vista, a dynamic index for ANNS that effectively addresses the challenges posed by imbalanced vector distributions. Vista improves the connectivity and retrieval efficiency of vectors with low  $k$ -NN connectivity, which are

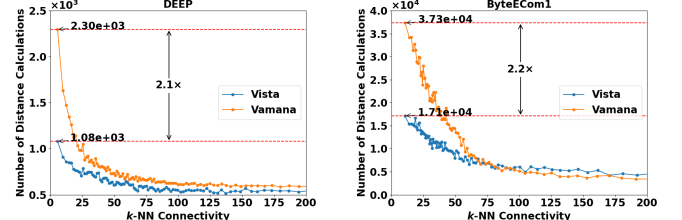


Fig. 11: Minimum number of distance calculations required to retrieve the ground truth vectors at different  $k$ -NN connectivity on two datasets. The ratio between the highest cost of Vamana and Vista is plotted.

typically difficult to retrieve. Experimental results demonstrate that Vista outperforms state-of-the-art methods such as Vamana and HCNG in efficiency. For instance, Vista achieved a 2.0 times acceleration at 0.92 recall on ByteECom1-100M over Vamana and a four-times acceleration over HCNG. Additionally, Vista efficiently scales with large datasets to achieve high-recall responses and demonstrates an advantage in handling complex datasets with numerous local clusters, which is crucial for industrial applications, while maintaining construction times comparable to leading baselines.

## REFERENCES

- [1] Hnswlib. <https://github.com/nmslib/hnswlib>, 2018.
- [2] Lsh-apg. <https://github.com/Jacyhust/LSH-APG>, 2023.
- [3] Parlayann. <https://github.com/cmuparlay/ParlayANN>, 2024.
- [4] J. Achiam, S. Adler, S. Agarwal, L. Ahmad, I. Akkaya, F. L. Aleman, D. Almeida, J. Altenschmidt, S. Altman, S. Anadkat, et al. Gpt-4 technical report. *arXiv preprint arXiv:2303.08774*, 2023.
- [5] L. Amsaleg, O. Chelly, T. Furou, S. Girard, M. E. Houle, K.-i. Kawarabayashi, and M. Nett. Estimating local intrinsic dimensionality. In *Proceedings of the 21th ACM SIGKDD International Conference on Knowledge Discovery and Data Mining*, pages 29–38, 2015.
- [6] F. André, A.-M. Kermarrec, and N. Le Scouarnec. Cache locality is not enough: High-performance nearest neighbor search with product quantization fast scan. In *42nd International Conference on Very Large Data Bases*, volume 9, page 12, 2016.
- [7] S. Arya and D. M. Mount. Approximate nearest neighbor queries in fixed dimensions. In *SODA*, volume 93, pages 271–280. Citeseer, 1993.
- [8] M. Aumüller, E. Bernhardsson, and A. Faithfull. Ann-benchmarks: A benchmarking tool for approximate nearest neighbor algorithms. In *International Conference on Similarity Search and Applications*, pages 34–49. Springer, 2017.
- [9] I. Azizi, K. Echihabi, and T. Palpanas. Elpis: Graph-based similarity search for scalable data science. *Proceedings of the VLDB Endowment*, 16(6):1548–1559, 2023.
- [10] S. Berchtold, C. Böhm, and H.-P. Kriegel. The pyramid-technique: towards breaking the curse of dimensionality. In *Proceedings of the 1998 ACM SIGMOD international conference on Management of data*, pages 142–153, 1998.
- [11] B. Bratić, M. E. Houle, V. Kurbalija, V. Oria, and M. Radovanović. The influence of hubness on nn-descent. *International Journal on Artificial Intelligence Tools*, 28(06):1960002, 2019.
- [12] T. Brown, B. Mann, N. Ryder, M. Subbiah, J. D. Kaplan, P. Dhariwal, A. Neelakantan, P. Shyam, G. Sastry, A. Askell, et al. Language models are few-shot learners. *Advances in neural information processing systems*, 33:1877–1901, 2020.
- [13] D. Caffagni, F. Cocchi, N. Moratelli, S. Sarto, M. Cornia, L. Baraldi, and R. Cucchiara. Wiki-llava: Hierarchical retrieval-augmented generation for multimodal llms. In *Proceedings of the IEEE/CVF Conference on Computer Vision and Pattern Recognition*, pages 1818–1826, 2024.
- [14] T. Cover and P. Hart. Nearest neighbor pattern classification. *IEEE transactions on information theory*, 13(1):21–27, 1967.
- [15] S. Dasgupta and Y. Freund. Random projection trees and low dimensional manifolds. In *Proceedings of the fortieth annual ACM symposium on Theory of computing*, pages 537–546, 2008.
- [16] Y. Ding, W. Fan, L. Ning, S. Wang, H. Li, D. Yin, T.-S. Chua, and Q. Li. A survey on rag meets llms: Towards retrieval-augmented large language models. *arXiv preprint arXiv:2405.06211*, 2024.
- [17] M. Dobson, Z. Shen, G. E. Blelloch, L. Dhulipala, Y. Gu, H. V. Simhadri, and Y. Sun. Scaling graph-based anns algorithms to billion-size datasets: A comparative analysis. *arXiv preprint arXiv:2305.04359*, 2023.
- [18] M. Dobson, Z. Shen, G. E. Blelloch, L. Dhulipala, Y. Gu, H. V. Simhadri, and Y. Sun. Scaling graph-based ANNS algorithms to billion-size datasets: A comparative analysis. *CoRR*, abs/2305.04359, 2023.
- [19] W. Dong, C. Moses, and K. Li. Efficient k-nearest neighbor graph construction for generic similarity measures. In *Proceedings of the 20th international conference on World wide web*, pages 577–586, 2011.
- [20] A. Fernández, S. García, F. Herrera, and N. V. Chawla. Smote for learning from imbalanced data: progress and challenges, marking the 15-year anniversary. *Journal of artificial intelligence research*, 61:863–905, 2018.
- [21] C. Fu, C. Wang, and D. Cai. High dimensional similarity search with satellite system graph: Efficiency, scalability, and unindexed query compatibility. *IEEE Transactions on Pattern Analysis and Machine Intelligence*, 44(8):4139–4150, 2021.
- [22] C. Fu, C. Xiang, C. Wang, and D. Cai. Fast approximate nearest neighbor search with the navigating spreading-out graph. *arXiv preprint arXiv:1707.00143*, 2017.
- [23] Y. Fu. Vista: Technical report. <https://github.com/YujianFu97/Vista-Technical-Report>, 2024.
- [24] A. Grover and J. Leskovec. node2vec: Scalable feature learning for networks. In *Proceedings of the 22nd ACM SIGKDD international conference on Knowledge discovery and data mining*, pages 855–864, 2016.
- [25] K. Hajebi, Y. Abbasi-Yadkori, H. Shahbazi, and H. Zhang. Fast approximate nearest-neighbor search with k-nearest neighbor graph. In *Twenty-Second International Joint Conference on Artificial Intelligence*, 2011.
- [26] W. Hamilton, Z. Ying, and J. Leskovec. Inductive representation learning on large graphs. *Advances in neural information processing systems*, 30, 2017.
- [27] P. Indyk and R. Motwani. Approximate nearest neighbors: towards removing the curse of dimensionality. In *Proceedings of the thirtieth annual ACM symposium on Theory of computing*, pages 604–613, 1998.
- [28] J. W. Jaromczyk and G. T. Toussaint. Relative neighborhood graphs and their relatives. *Proceedings of the IEEE*, 80(9):1502–1517, 1992.
- [29] S. Jayaram Subramanya, F. Devvrit, H. V. Simhadri, R. Krishnawamy, and R. Kadekodi. Rand-nsg: Fast accurate billion-point nearest neighbor search on a single node. In H. Wallach, H. Larochelle, A. Beygelzimer, F. d’Alché-Buc, E. Fox, and R. Garnett, editors, *Advances in Neural Information Processing Systems 32*, pages 13771–13781. Curran Associates, Inc., 2019.
- [30] J. Johnson, M. Douze, and H. Jégou. Billion-scale similarity search with gpus. *IEEE Transactions on Big Data*, 2019.
- [31] J. Kleinberg. The small-world phenomenon: An algorithmic perspective. In *Proceedings of the thirty-second annual ACM symposium on Theory of computing*, pages 163–170, 2000.
- [32] M. Li, Y.-G. Wang, P. Zhang, H. Wang, L. Fan, E. Li, and W. Wang. Deep learning for approximate nearest neighbour search: A survey and future directions. *IEEE Transactions on Knowledge and Data Engineering*, 35(9):8997–9018, 2022.
- [33] W. Li, Y. Zhang, Y. Sun, W. Wang, M. Li, W. Zhang, and X. Lin. Approximate nearest neighbor search on high dimensional data—experiments, analyses, and improvement. *IEEE Transactions on Knowledge and Data Engineering*, 2019.
- [34] P.-C. Lin and W.-L. Zhao. Graph based nearest neighbor search: Promises and failures. *arXiv preprint arXiv:1904.02077*, 2019.
- [35] T. Liu, A. Moore, K. Yang, and A. Gray. An investigation of practical approximate nearest neighbor algorithms. *Advances in neural information processing systems*, 17, 2004.
- [36] X. Liu, Y. Zheng, Z. Du, M. Ding, Y. Qian, Z. Yang, and J. Tang. Gpt understands, too. *AI Open*, 2023.
- [37] Y. Liu, D. Zhang, G. Lu, and W.-Y. Ma. A survey of content-based image retrieval with high-level semantics. *Pattern recognition*, 40(1):262–282, 2007.
- [38] D. G. Lowe. Distinctive image features from scale-invariant keypoints. *International journal of computer vision*, 60:91–110, 2004.
- [39] K. Lu, M. Kudo, C. Xiao, and Y. Ishikawa. Hvs: hierarchical graph structure based on voronoi diagrams for solving approximate nearest neighbor search. *Proceedings of the VLDB Endowment*, 15(2):246–258, 2021.
- [40] Y. Malkov, A. Ponomarenko, A. Logvinov, and V. Krylov. Approximate nearest neighbor algorithm based on navigable small world graphs. *Information Systems*, 45:61–68, 2014.
- [41] Y. A. Malkov and D. A. Yashunin. Efficient and robust approximate nearest neighbor search using hierarchical navigable small world graphs. *IEEE transactions on pattern analysis and machine intelligence*, 2018.
- [42] M. D. Manohar, Z. Shen, G. Blelloch, L. Dhulipala, Y. Gu, H. V. Simhadri, and Y. Sun. Parlayann: Scalable and deterministic parallel graph-based approximate nearest neighbor search algorithms. In *Proceedings of the 29th ACM SIGPLAN Annual Symposium on Principles and Practice of Parallel Programming*, pages 270–285, 2024.
- [43] T. Mikolov, I. Sutskever, K. Chen, G. S. Corrado, and J. Dean. Distributed representations of words and phrases and their compositionality. *Advances in neural information processing systems*, 26, 2013.
- [44] J. V. Munoz, M. A. Gonçalves, Z. Dias, and R. d. S. Torres. Hierarchical clustering-based graphs for large scale approximate nearest neighbor search. *Pattern Recognition*, 96:106970, 2019.
- [45] Y. Peng, B. Choi, T. N. Chan, J. Yang, and J. Xu. Efficient approximate nearest neighbor search in multi-dimensional databases. *Proceedings of the ACM on Management of Data*, 1(1):1–27, 2023.
- [46] J. Pennington, R. Socher, and C. D. Manning. Glove: Global vectors for word representation. <https://nlp.stanford.edu/projects/glove/>, 2014.
- [47] B. Perozzi, R. Al-Rfou, and S. Skiena. Deepwalk: Online learning of social representations. In *Proceedings of the 20th ACM SIGKDD international conference on Knowledge discovery and data mining*, pages 701–710, 2014.

- [48] A. Radford, K. Narasimhan, T. Salimans, I. Sutskever, et al. Improving language understanding by generative pre-training. 2018.
- [49] A. Radford, J. Wu, R. Child, D. Luan, D. Amodei, I. Sutskever, et al. Language models are unsupervised multitask learners. *OpenAI blog*, 1(8):9, 2019.
- [50] M. Radovanović, A. Nanopoulos, and M. Ivanović. Nearest neighbors in high-dimensional data: The emergence and influence of hubs. In *Proceedings of the 26th Annual International Conference on Machine Learning*, pages 865–872, 2009.
- [51] M. Radovanovic, A. Nanopoulos, and M. Ivanovic. Hubs in space: Popular nearest neighbors in high-dimensional data. *Journal of Machine Learning Research*, 11(sept):2487–2531, 2010.
- [52] M. Reza, B. Ghahremani, and H. Naderi. A survey on nearest neighbor search methods. *International Journal of Computer Applications*, 95(25):39–52, 2014.
- [53] A. Salemi and H. Zamani. Evaluating retrieval quality in retrieval-augmented generation. In *Proceedings of the 47th International ACM SIGIR Conference on Research and Development in Information Retrieval*, pages 2395–2400, 2024.
- [54] J. B. Schafer, D. Frankowski, J. Herlocker, and S. Sen. Collaborative filtering recommender systems. In *The adaptive web: methods and strategies of web personalization*, pages 291–324. Springer, 2007.
- [55] C. Szegedy, W. Liu, Y. Jia, P. Sermanet, S. Reed, D. Anguelov, D. Erhan, V. Vanhoucke, and A. Rabinovich. Going deeper with convolutions. In *Proceedings of the IEEE conference on computer vision and pattern recognition*, pages 1–9, 2015.
- [56] J. Tang, M. Qu, M. Wang, M. Zhang, J. Yan, and Q. Mei. Line: Large-scale information network embedding. In *Proceedings of the 24th international conference on world wide web*, pages 1067–1077, 2015.
- [57] Y. Tian, X. Zhao, and X. Zhou. Db-lsh 2.0: Locality-sensitive hashing with query-based dynamic bucketing. *IEEE Transactions on Knowledge and Data Engineering*, 2023.
- [58] L. Van der Maaten and G. Hinton. Visualizing data using t-sne. *Journal of machine learning research*, 9(11), 2008.
- [59] H. Wang, Z. Wang, W. Wang, Y. Xiao, Z. Zhao, and K. Yang. A note on graph-based nearest neighbor search. *arXiv preprint arXiv:2012.11083*, 2020.
- [60] J. Wang, J. Wang, G. Zeng, R. Gan, S. Li, and B. Guo. Fast neighborhood graph search using cartesian concatenation. In *Proceedings of the IEEE International Conference on Computer Vision*, pages 2128–2135, 2013.
- [61] M. Wang, X. Xu, Q. Yue, and Y. Wang. A comprehensive survey and experimental comparison of graph-based approximate nearest neighbor search. *arXiv preprint arXiv:2101.12631*, 2021.
- [62] Z. Wang, P. Wang, T. Palpanas, and W. Wang. Graph-and tree-based indexes for high-dimensional vector similarity search: Analyses, comparisons, and future directions. *IEEE Data Eng. Bull.*, 46(3):3–21, 2023.
- [63] J. Wei, B. Peng, X. Lee, and T. Palpanas. Det-lsh: A locality-sensitive hashing scheme with dynamic encoding tree for approximate nearest neighbor search. *arXiv preprint arXiv:2406.10938*, 2024.
- [64] X. Zhao, Y. Tian, K. Huang, B. Zheng, and X. Zhou. Towards efficient index construction and approximate nearest neighbor search in high-dimensional spaces. *Proceedings of the VLDB Endowment*, 16(8):1979–1991, 2023.

## APPENDIX

### A. Discussion on distribution-related parameter $\alpha$ and $C$

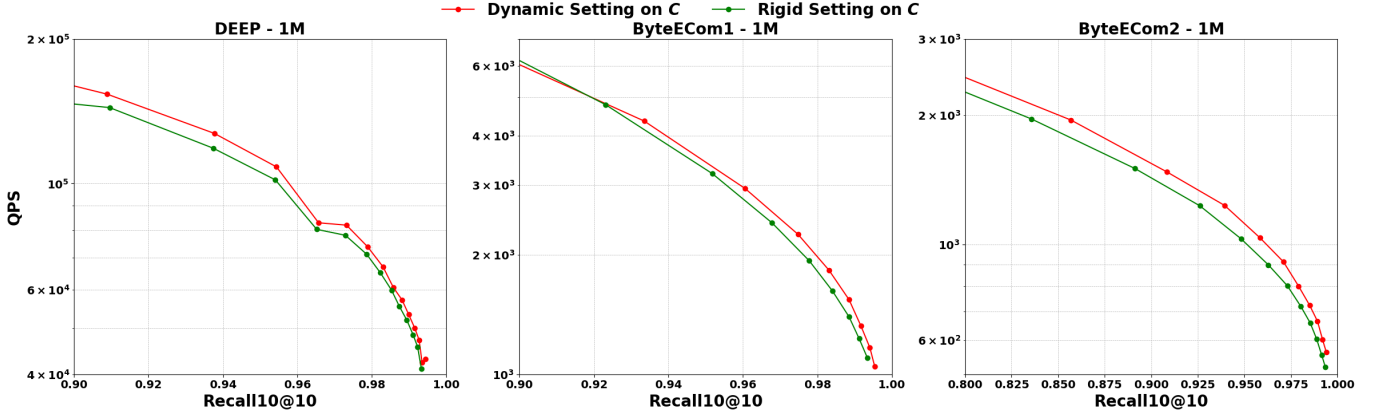


Fig. 12: Comparison of parameter settings for the search list size  $C$ . Vista’s dynamic setting compensates for vectors with low  $k$ -NN connectivity by enabling more neighbors for edge construction, while the rigid setting applies a fixed configuration to all vectors. For a fair comparison, the average degree in the resulting graph is kept the same for both settings. Vista’s dynamic approach consistently outperforms the rigid setting across all datasets in terms of efficiency.

#### 1. Evaluation on $C$ :

To demonstrate the effectiveness of distribution-aware parameter settings and compensation for low-connectivity vectors, we compare Vista’s dynamic setting for  $C_i$  with the rigid, fixed setting used in traditional graph indexes. In the dynamic approach,  $C_i$  is set to  $K + (K - \min(K, p_i))$ , while in the rigid approach,  $C_i$  is manually adjusted to maintain the same average degree as the dynamic setting. We evaluate the search performance of both strategies on three million-scale datasets, as shown in Figure 12. The results indicate that our dynamic compensation strategy consistently outperforms the rigid setting at high recall levels, confirming the efficiency of our approach.

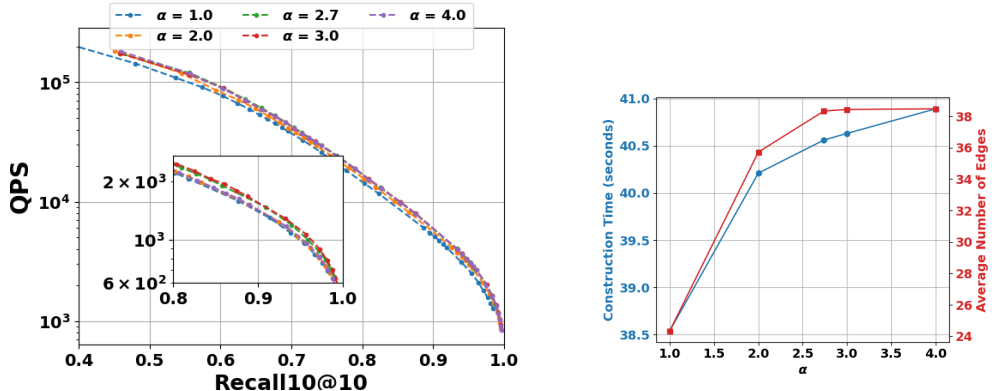


Fig. 13: Comparison on construction parameter settings on  $\alpha$  on ByteECom1 - 1M dataset.  $\alpha = 2.7$  is the learned setting based on the dataset distribution, while the other parameters are manually set. The learned setting achieves the near-optimal search performance with lower construction cost than other settings with comparable search performance, e.g.  $\alpha = 3.0$ .

#### 2. Evaluation on $\alpha$ :

We assess the effectiveness of the learned  $\alpha$  setting, derived from vector distribution, by comparing it with manual settings on the DEEP-1M, ByteECom1-1M, and ByteECom2-1M datasets. The evaluation covers both construction and retrieval performance and results are presented in Figures 13, 14, and 15. In each figure, the right panels illustrate construction cost while the left panels show search performance with subfigures highlighting the high-recall range for clearer visualization. Our evaluation results indicate that the learned  $\alpha$  achieves optimal or near-optimal search performance with lower construction costs than other settings with comparable performance, validating the effectiveness of our  $\alpha$  learning process.

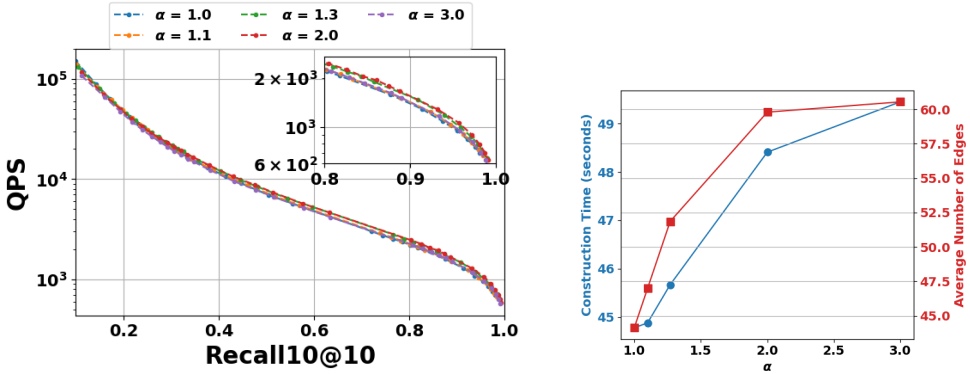


Fig. 14: Comparison on construction parameter settings on  $\alpha$  on ByteECom2 - 1M dataset.  $\alpha = 1.3$  is the learned setting based on the dataset distribution, while the other parameters are manually set. The learned setting achieves the best search performance with lower construction cost than other settings with comparable search performance, e.g.  $\alpha = 2.0$ .

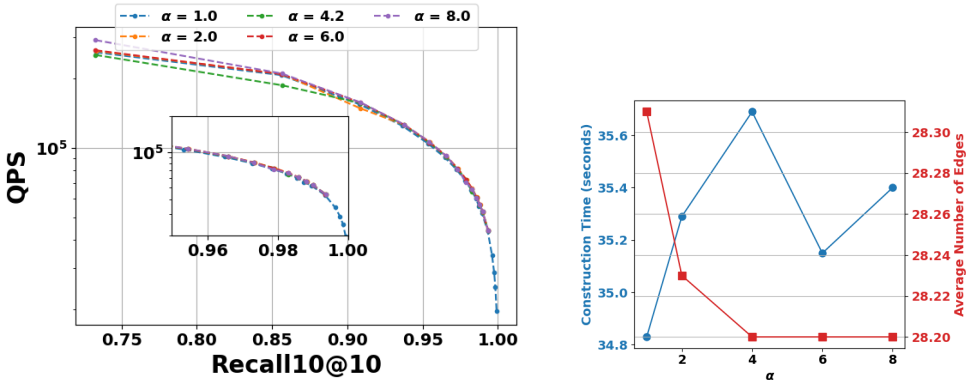


Fig. 15: Comparison on construction parameter settings on  $\alpha$  on DEEP - 1M dataset.  $\alpha = 4.2$  is the learned setting based on the dataset distribution, while the other parameters are manually set. For this dataset, the differences in construction and search performance across various  $\alpha$  settings are minimal.

### B. Discussion on hubness

First, we clarify the definition of hubs and their importance. Hubs are vectors with a disproportionately large number of out-edges in proximity ANNS graphs and significantly influence search efficiency. 'Good' hubs direct the search toward key regions, improving both efficiency and accuracy, while 'bad' hubs lead to unnecessary computations by connecting to irrelevant points. Effective hub management is therefore crucial in designing graph indices.

Traditional ANNS graph methods like HNSW, HCNNG, and Vamana use a brute-force approach to suppress all hubs by imposing user-defined fixed bounds based solely on edge count. This approach overlooks the potential routing benefits that some hubs can offer. Additionally, as indicated in Equation 3, pruning hubs with fixed upper bounds on graph edges can create connectivity problems in high-dimensional, skewed datasets, leaving some poorly connected vectors with limited or no paths.

In contrast, Vista acknowledges the importance of preserving certain hubs for effective routing, particularly for vectors with low  $k$ -NN connectivity. By employing an adaptive strategy—dynamic edge exchange—we retain beneficial 'good' hubs for routing while minimizing unnecessary connections to irrelevant points through the distance-based RNG strategy on edges. This approach enhances search efficiency while maintaining the benefits of key hubs. The following experiments support these findings.

Second, we evaluate Vista's hub control strategy in comparison with the traditional rigid approach in terms of edge structure and search efficiency.

To assess the impact of hub control strategies on index structure and retrieval performance, we conduct experiments using the two strategies in Vista. Both approaches use the same initialized approximate  $k$ -NN graph on three real-world datasets with 1 million vectors, following identical candidate generation and edge selection processes. The key difference lies in how each strategy manages the final size of out-edges for each vector to control hubs in Vista, with all other configurations as specified in Section V-A. We compare the rigid and flexible strategies in terms of edge distribution and search efficiency, demonstrating

that Vista’s dynamic hub control method is more effective.

*Strategy 1.* Rigid edge size control: If the number of out-edges exceeds a fixed upper bound, only the closest edges are preserved. The upper bound is set to  $K = 50$ , i.e. the approximate number of neighbors computed during initialization.

*Strategy 2.* Dynamic edge size control: We follow the dynamic edge exchange mechanism proposed in Algorithm 6.

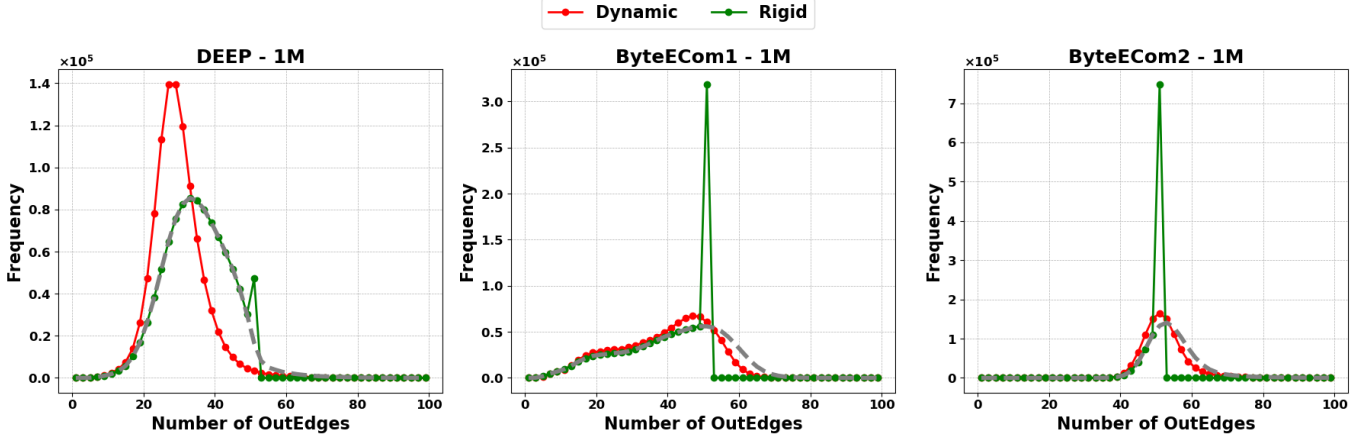


Fig. 16: Frequency of out-degree on various datasets. The grey line represents no hubness control, meaning no edges are pruned. The rigid strategy uses  $K = 50$  as the upper bound for edge pruning.

In this experiment, we analyze the edge distribution in graphs constructed using two different strategies. Figure 16 shows the out-degree distribution across various datasets, with the grey dotted line representing the original edge distribution without pruning. The traditional rigid method limits edges once the out-degree exceeds a set threshold ( $K = 50$ ), resulting in zero frequency beyond 50 (green line) and causing many vectors to reach the maximum out-degree of 50.

In contrast, our dynamic strategy adjusts out-degree control based on both vector and edge distribution, focusing pruning efforts on vectors with higher out-degrees (as described in Algorithm 6, where edge exchanges occur from vectors with higher to lower out-degrees). This approach reduces—but does not entirely eliminate—vectors with high out-degrees, resulting in a higher proportion of vectors with moderate edge counts. It also retains key edges for vectors with low  $k$ -NN connectivity, while the traditional method removes these edges, negatively impacting accuracy for poorly connected vectors.

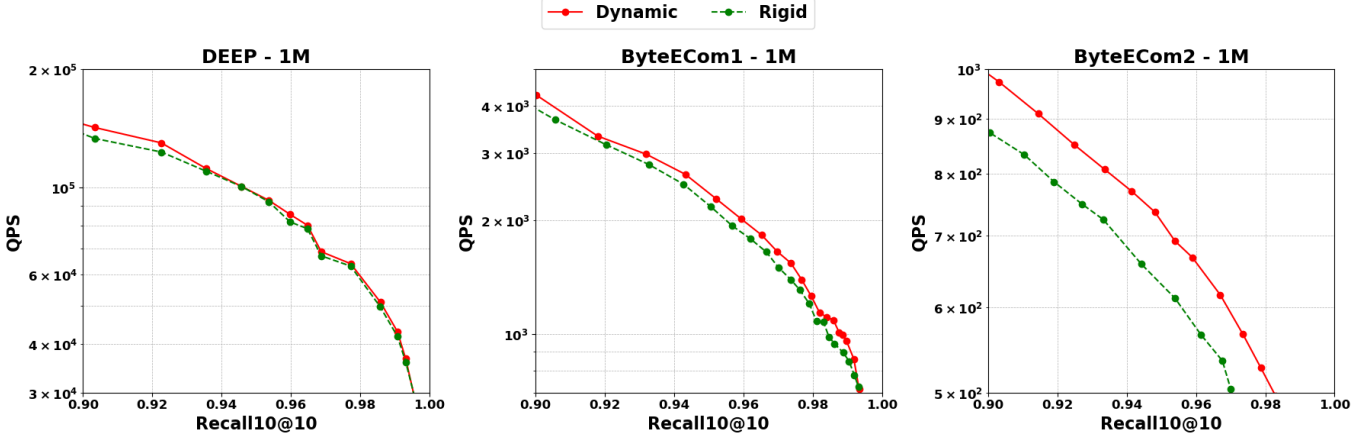


Fig. 17: Search performance comparison between two strategies. Our dynamic strategy is more efficient on all datasets.

In this experiment, we compare the search efficiency of two strategies across three datasets in terms of recall and speed, as shown in Figure 17. Our dynamic strategy consistently achieves equal or better speed and accuracy at high recall levels across all datasets. This improvement is particularly notable in the two GNN industrial datasets, where the rigid hub control strategy removes many edges from high out-degree vectors, increasing retrieval costs for vectors with low  $k$ -NN connectivity.

#### C. Discussion on edge compensation for low connectivity vectors

We establish approximate theoretical bounds and estimations in Vista to demonstrate that it avoids introducing an excessive number of in-edges for low-connectivity vectors and prevents excessive skewness in the graph structure. We aim to demonstrate that while our design compensates for constructing in-edges for vectors with low  $k$ -NN connectivity, the in-degree of these

vectors (with  $k$ -NN connectivity  $< K$ ) is approximately upper-bounded by a scalar that is smaller than the in-degree upper bound for vectors with high  $k$ -NN connectivity ( $> K$ ).

Using the notations defined in Table II, we begin the analysis with Equation 1, which describes the in-edges of vectors in traditional graph indexes:

$$\begin{aligned}\mathcal{I}(v_i) &= \mathcal{P}(v_i, n, (\mathcal{S}(v_i, \mathcal{N}(v_i, m)))) \\ &\cup \mathcal{P}(v_i, n, \{v_j \mid v_i \in \mathcal{S}(v_j, \mathcal{N}(v_j, m))\})\end{aligned}$$

In Vista, we apply an element-wise upper bound on the number of edge candidates, combined with distribution-based edge pruning, as outlined in Section IV. For a given vector  $v_i$ , the upper bound on the number of edge candidates is defined as  $m_i = \alpha \cdot C_i = \alpha \cdot (K + (K - \min(K, p_i)))$ . The edge pruning process, represented by  $\mathcal{T}(v_i, \mathcal{X})$ , selects a subset of vectors from  $\mathcal{X}$  such that  $v_i$  appears among the outgoing edges generated by the dynamic edge exchange (Algorithm 6) of vectors in  $\mathcal{X}$ . As a result, the in-edges of vector  $v_i$  in the Vista graph, denoted by  $\mathcal{I}'(v_i)$ , are:

$$\begin{aligned}\mathcal{I}'(v_i) &= \mathcal{T}(v_i, (\mathcal{S}(v_i, \mathcal{N}(v_i, \alpha \cdot C_i)))) \\ &\cup \mathcal{T}(v_i, \{v_j \mid v_i \in \mathcal{S}(v_j, \mathcal{N}(v_j, \alpha \cdot C_i))\})\end{aligned}$$

Since the RNG-based edge selection process is highly dependent on vector distribution, we start with a simplified scenario where no edge pruning occurs during the edge selection  $\mathcal{S}$ . In this scenario, we present the following:

**1. The in-edges for vectors with low  $k$ -NN connectivity ( $< K$ ) are approximately bounded by a value determined solely by the scalar parameter  $K$ .**

**2. The upper bound of in-edges for vectors with high  $k$ -NN connectivity ( $> K$ ) is greater than that for vectors with low  $k$ -NN connectivity.**

In this case, we have  $\mathcal{S}(v_i, \mathcal{X}) = \mathcal{X}$ . Also, from the definition of  $\alpha$  in Equation 5,  $\alpha = K/P = 1.0$ . Thus we have:

$$\begin{aligned}\mathcal{I}'(v_i) &= \mathcal{T}(v_i, \mathcal{N}(v_i, C_i)) \\ &\cup \mathcal{T}(v_i, \{v_j \mid v_i \in \mathcal{N}(v_j, C_i)\}) \\ &\subseteq \mathcal{N}(v_i, C_i) \cup \{v_j \mid v_i \in \mathcal{N}(v_j, C_i)\}\end{aligned}$$

From the above equation, the first set represents the neighboring vectors of  $v_i$ , while the second set consists of vectors  $v_j$  that consider  $v_i$  as an edge candidate. Without any assumptions regarding the distribution of  $v_j$ , we approximate the size of the second set of  $v_i$  as  $|\mathcal{M}(v_i, K)|$ . We have already established the  $k$ -NN relationship with  $k = K$ , where  $|\mathcal{M}(v_i, K)| = p_i$ . Therefore, considering the size of in-edges of  $v_i$ , we have:

$$\begin{aligned}|\mathcal{I}'(v_i)| &\leq |\mathcal{N}(v_i, C_i)| + |\{v_j \mid v_i \in \mathcal{N}(v_j, C_i)\}| \\ &\approx |\mathcal{N}(v_i, C_i)| + |\mathcal{M}(v_i, K)| \\ &= 2 \cdot K - \min(K, p_i) + p_i\end{aligned}$$

From the above expression, for vectors with low  $k$ -NN connectivity ( $p_i < K$ ), the upper bound for in-edges is  $2 \cdot K$ . In contrast, for vectors with high  $k$ -NN connectivity, the upper bound is  $K + p_i > 2 \cdot K$ .

In the second case, when considering the RNG strategy for edge selection, we have  $\alpha > 1.0$ , and  $\alpha \cdot C_i$  edge candidates are generated for each vector. Given that the edge selection process is significantly influenced by the vector distribution, we provide an estimation of the upper bound of in-degree based on approximate assumptions for vectors.

**Assumption 1:** The RNG edge selection process selects edges for vectors in a linear manner, meaning that the number of resulting edges is  $\frac{1}{\alpha}$  of the total number of edge candidates.

**Assumption 2:** The  $k$ -NN connectivity remains stable as  $k$  increases, i.e.,  $|\mathcal{M}(v_i, \alpha \cdot K)| \approx \alpha \cdot |\mathcal{M}(v_i, K)|$ .

Both assumptions are highly dependent on the value of  $\alpha$ . In our applications,  $\alpha$  is relatively small, i.e.,  $< 5.0$ , which makes these assumptions approximately valid. Based on these assumptions, we have:

**1. The in-edges for vectors with low  $k$ -NN connectivity ( $< K$ ) are approximately bounded by a value related to scalar parameters  $K$  and  $\alpha$ .**

**2. The estimated bound on the in-degree of vectors with high  $k$ -NN connectivity is higher than that of vectors with low  $k$ -NN connectivity.**

Consider above assumptions in  $\mathcal{I}'(v_i)$ , we have:

$$\begin{aligned}
|\mathcal{I}'(v_i)| &\leq |\mathcal{T}(v_i, (\mathcal{S}(v_i, \mathcal{N}(v_i, \alpha \cdot C_i))))| \\
&\quad + |\mathcal{T}(v_i, \{v_j \mid v_i \in \mathcal{S}(v_j, \mathcal{N}(v_j, \alpha \cdot C_i))\})| \\
&\leq |\mathcal{S}(v_i, \mathcal{N}(v_i, \alpha \cdot C_i))| \\
&\quad + |\{v_j \mid v_i \in \mathcal{S}(v_j, \mathcal{N}(v_j, \alpha \cdot C_i))\}| \\
&\approx \alpha \cdot C_i + \alpha \cdot p_i = \alpha \cdot (C_i + p_i) \\
&= \alpha \cdot (2 \cdot K - \min(K, p_i) + p_i)
\end{aligned}$$

From the above expression, for vectors with low  $k$ -NN connectivity ( $p_i < K$ ), the approximate upper bound for in-edges is  $2 \cdot \alpha \cdot K$ . For vectors with high  $k$ -NN connectivity, the upper bound is  $\alpha \cdot (K + p_i) > 2 \cdot \alpha \cdot K$ , which is larger than the approximate bound for vectors with low  $k$ -NN connectivity.

#### D. Information on synthetic datasets

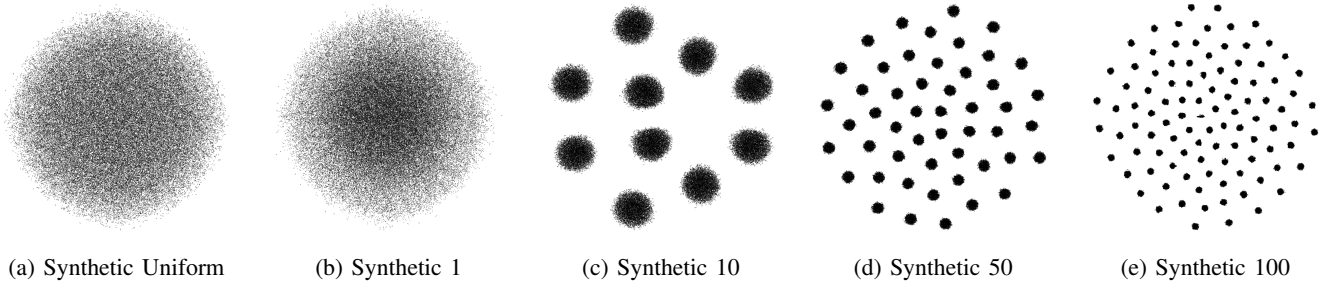


Fig. 18: Visualization of Synthetic datasets with t-SNE.

We use  $t$ -SNE to visualize the synthetic datasets in 2-D, as shown in the appendix of our technical report. Figure 18 confirms that the datasets exhibit uniform or Gaussian distributions, with well-defined clusters for multi-cluster datasets. We also analyze  $k$ -NN connectivity distribution across datasets, visualized in Figure 19. Uniform datasets have a higher proportion of vectors with high  $k$ -NN connectivity, while Gaussian datasets contain more vectors with low  $k$ -NN connectivity. Datasets with more clusters show greater  $k$ -NN connectivity among most vectors but fewer vectors with low connectivity. These distinct distributions make the datasets suitable for stress-testing.

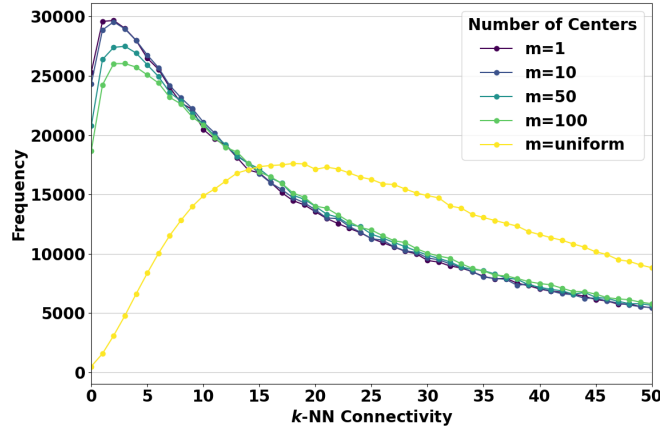


Fig. 19: Distribution of  $k$ -NN connectivity of various datasets.

#### E. Discussion on vector skewness on various ANNS indexes

First, we examine the impact of dataset imbalance on the retrieval performance of various ANNS indexes. As recommended by ANN-Benchmark [8], tree, hashing, and graph methods are suitable for large-scale ANNS. Hence we include the state-of-the-art graph-based method Vamana [29], the tree-based method Faiss-ivfpqfs [6], and the hashing-based method DET-LSH [63]. We start by analyzing the distribution of search costs for database vectors, measured by the number of distance calculations

needed to identify the correct ground truth vectors. The frequency distribution of search costs per vector is shown in Figure 20.

The results indicate that Faiss and DET-LSH exhibit a more concentrated distribution of search costs, while Vamana has a wider range. This suggests that the computation cost in graph-based searches can vary significantly, depending on the distribution of the query, ground truth, and index structure. As a result, it is meaningful to explore ways to improve efficiency for retrieving extremely hard-to-find vectors in graph-based indexes. In contrast, since Faiss and DET-LSH have more consistent search costs across queries, optimizing query efficiency based on cost distribution is less impactful than for graph-based indexes.

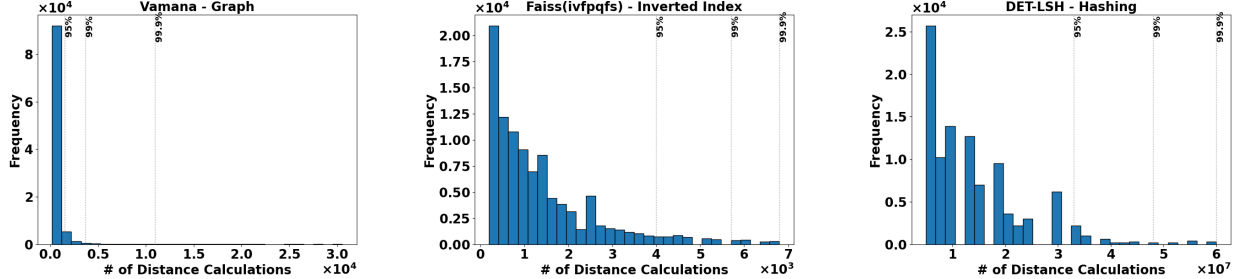


Fig. 20: Distribution of search cost, i.e. number of distance calculations of various indexes on DEEP dataset. Dotted lines indicate the percentage of vectors that have search costs lower than the threshold marked by the line.

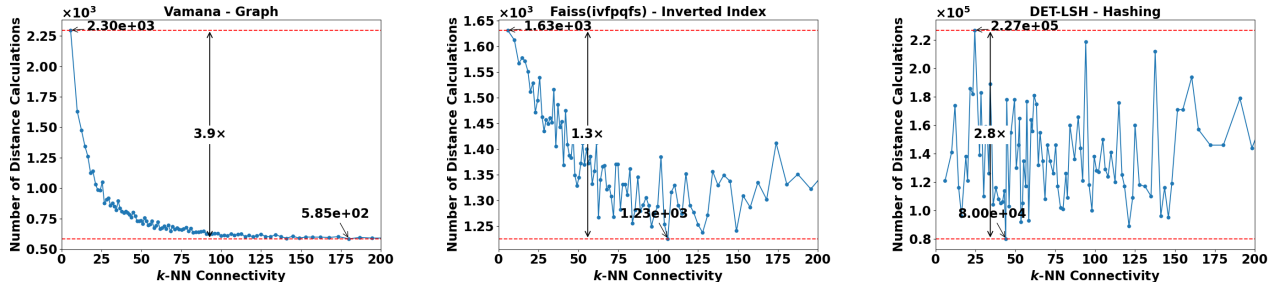


Fig. 21: Distribution of search cost with  $k$ -NN connectivity on various types of indexes.

Second, we analyze the relationship between search costs and  $k$ -NN connectivity for tree-based and hashing-based indexes, using  $k$ -NN connectivity as an indicator of search difficulty. Figure 21 plots search costs of ground truth vectors against their  $k$ -NN connectivity on the DEEP-1M dataset, with each point representing the center of 1,000 nearby points for clarity.

The results show a clear trend for the graph-based index: search costs decrease as  $k$ -NN connectivity increases. In contrast, the tree-based index (Faiss) exhibits high search costs for vectors with very low  $k$ -NN connectivity (e.g., < 30), while showing no clear pattern for other vectors. This is likely due to the sparse distribution of low-connectivity vectors, making them difficult to allocate to appropriate clusters in the space partitioning process. For the hashing-based method (DET-LSH), there is no evident relationship between  $k$ -NN connectivity and search cost, indicating that both tree-based and hashing-based methods are not particularly sensitive to  $k$ -NN connectivity in retrieval tasks.

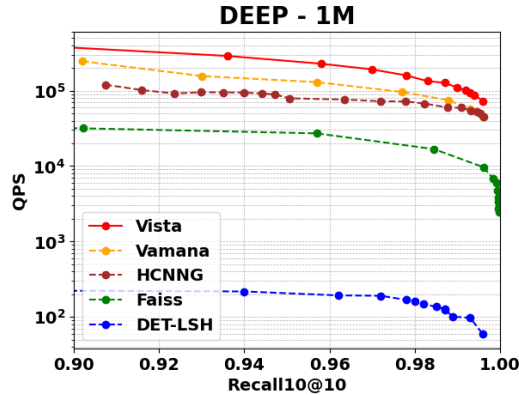


Fig. 22: Search performance comparison between various types of indexes on DEEP-1M dataset.

Lastly, we focus on graph-based approaches, which are the leading solutions in industrial-grade applications due to their high

efficiency and accuracy. This observation is supported by numerous benchmarks on datasets ranging from millions to billions in scale [8], [9], [33], [59], [61], which we validate in our evaluation. We compare the graph-based methods, tree-based index (IVFPQFS) [6] in the Faiss library [30] and the hashing-based method (DET-LSH [63]) on million-scale datasets, presenting retrieval performance in Figure 22. On the DEEP-1M dataset, graph-based methods, including Vista, Vamana, and HCNNG, achieve significantly faster search speeds than tree-based and hashing-based methods, particularly at high recall levels, making them more suitable for industrial applications at ByteDance.

#### F. Discussion on parameter $L$ and $R$

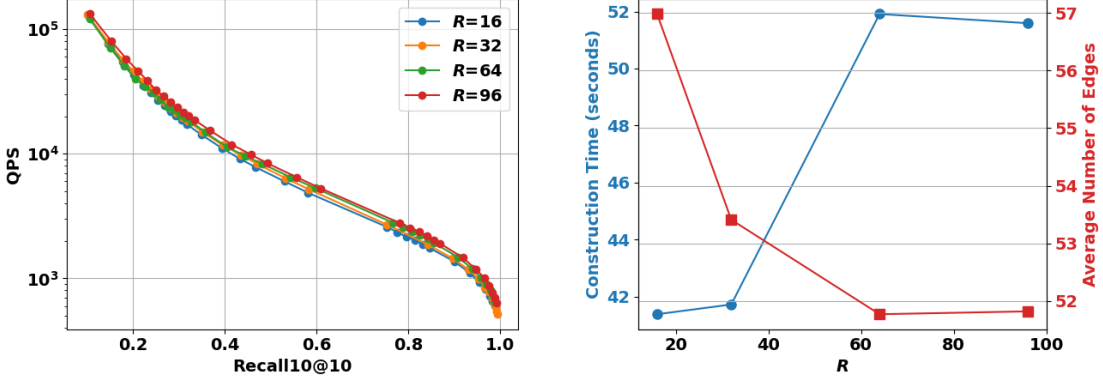


Fig. 23: Comparison on construction parameter settings on  $R$ .

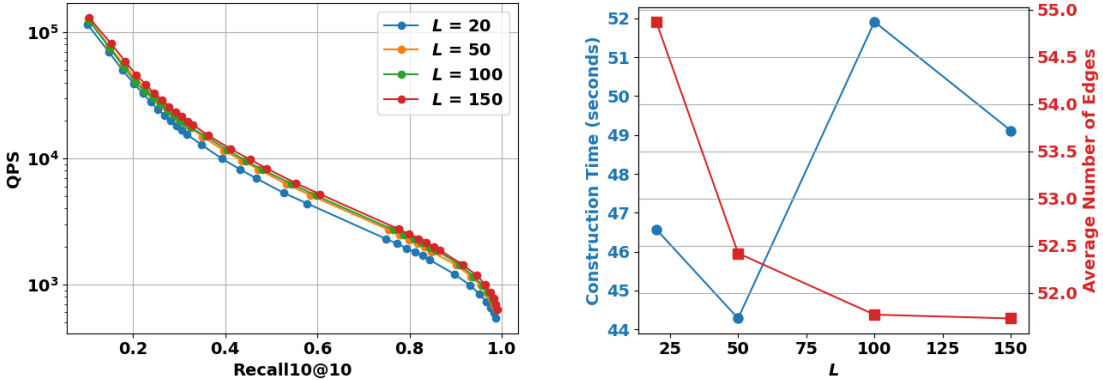


Fig. 24: Comparison on construction parameter settings on  $L$ .

The user-defined parameters in Algorithm 1 and Table V include the maximum leaf size in the random projection tree (RPT)  $L$ , the number of RPTs  $R$ , and the number of nearest neighbors for initialization  $K$ . Among these,  $K$  is the most crucial, as it directly impacts graph edge formation; its evaluation is discussed in Section V-E. Here, we focus on the impact of  $R$  and  $L$  on construction and retrieval performance. These parameters influence RPT construction, which initializes the approximate  $k$ -NN graph for further Vista graph construction and query retrieval.

#### 1. Evaluation on $R$ :

Figure 23 shows that increasing  $R$  slightly enhances search performance, as reflected by an upward shift in QPS. Higher values of  $R$  (e.g., 64 and 96) consistently deliver better QPS at high recall levels compared to lower values (e.g., 16 and 32), indicating that a larger  $R$  expands the pool of search candidates and improves retrieval.

However, increasing  $R$  also leads to trade-offs: both construction time and the average number of edges in the index rise. Notably, construction time spikes between  $R = 40$  and  $R = 60$ , while the average number of edges peaks at  $R = 60$ . Beyond this, both metrics plateau, showing diminishing returns relative to the increased costs. These results suggest that while larger  $R$  values enhance search efficiency, they also require more computational resources, requiring a balance based on application needs.

#### 2. Evaluation on $L$ :

Figure 24 shows that increasing  $L$ , which controls leaf size in the RPT, generally improves search performance, especially at high recall levels. Higher values of  $L$  (e.g., 100 and 150) consistently deliver better QPS compared to lower values (e.g., 20 and 50), indicating that larger leaf sizes accommodate more candidates per search iteration.

The figure also shows that construction time remains stable across different  $L$  values, with no clear trend. Meanwhile, the average number of edges slightly decreases as  $L$  increases, resulting in a more compact index. This suggests that larger  $L$  values can improve search efficiency without significantly affecting construction costs, allowing for balanced performance based on application requirements.

#### *G. Notes on Implementation*

The implementation of the ANNS index is crucial for its performance in both the construction and retrieval phases. We follow the non-lock design introduced in ParlayANN [18] for edge candidate acquisition and edge selection. Instead of using locks to handle conflicts in parallelism, we process vectors in small batches, each set to 2% of the total number of vectors. For each batch, we launch the search task for edge candidate acquisition, followed by edge selection and update. This ensures that edge information is either read or written in a single stage, allowing us to remove locks.

In the retrieval process, graph indexes with beam search require a structure to record the visiting status of all vectors to avoid redundant distance calculations. Allocating memory for a list of boolean variables for all database vectors is expensive for large-scale datasets, especially in high-parallelism scenarios. Instead, we allocate memory for visit status lists before starting the search and re-initialize the lists after retrieval.

#### *H. Complexity in Vista*

We analyze the complexity of the Vista index as follows:**Search Complexity:** The time complexity for the retrieval task is the same as other variants of RNG, such as HNSW and NSG, i.e.,  $O(\log(N))$ .**Construction Complexity:** The construction complexity is the sum of the complexities of all stages. The initialization process, including partitioning the dataset and generating approximate  $k$  nearest neighbors, has a complexity of  $O(n \cdot (N \cdot \log(\frac{N}{m}) + N \cdot m))$ . The edge candidate acquisition requires searching the entire dataset for each vector, resulting in a complexity of  $O(N \cdot \log(N))$ . Selecting and exchanging the edges with the RNG rule takes  $O(N \cdot (C + \alpha \cdot k)^2)$ . Overall, the complexity of building Vista is the sum of all components, i.e.,  $O(N \cdot (n \cdot \log(\frac{N}{m}) + n \cdot m + \log(N) + (C + \alpha \cdot k)^2)) \approx O(N \cdot \log(N))$ .